New Phenomena in Gamma-Ray Strength Functions

Ronald Schwengner

Institute of Radiation Physics, Helmholtz-Zentrum Dresden-Rossendorf, 01328 Dresden, Germany

- *Experiments:*
  - Photon scattering using bremsstrahlung at γELBE and quasi-monoenergetic polarized γ rays at HIγS
  - Data analysis
- *E1 strength in the pygmy region*
- *M1 strength in the spin-flip region*
- *Low-energy M1 strength*

HZDR

HELMHOLTZ ZENTRUM DRESDEN ROSSENDORF

Photonuclear and radiative-capture reactions

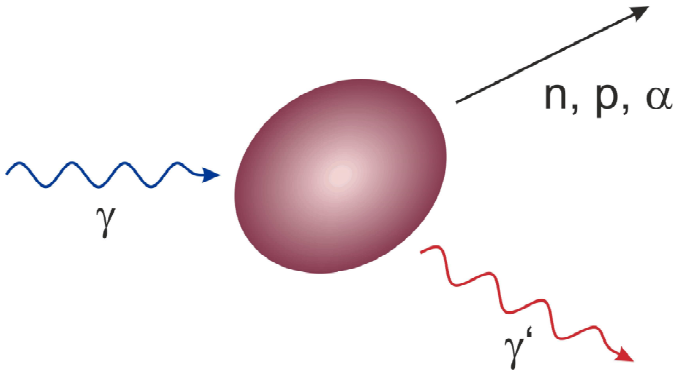

Excitation and deexcitation of the nucleus by γ rays:

- Statistical models applied to describe reaction rates at high excitation energy and high level density.
- γ-ray strength functions used to describe average transition strengths in a certain energy range.
- Understanding of the properties of γ-ray strength functions attracts increasing interest.

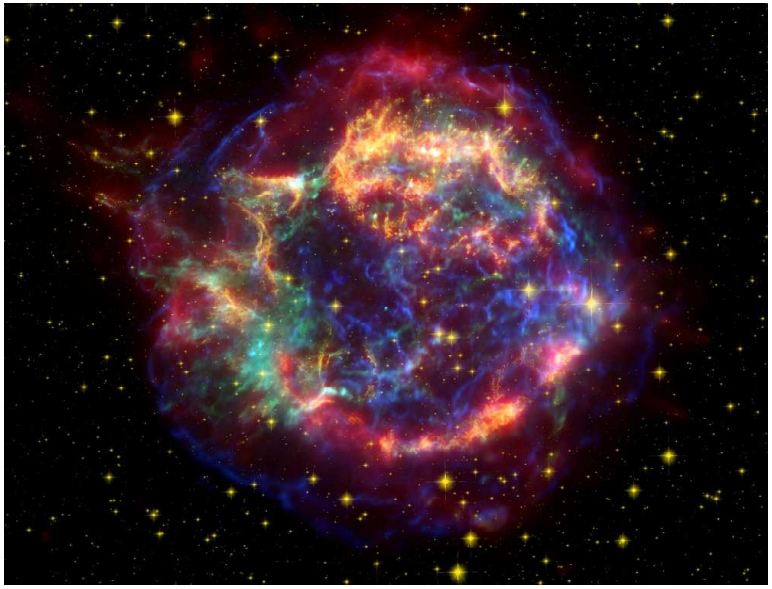

Cassiopeia A (gallery.spitzer.caltech.edu)

Application:

- Photonuclear and radiative-capture reactions play a central role in the synthesis of the elements in various stellar environments.

Effect of enhanced low-energy dipole strength in the r-process

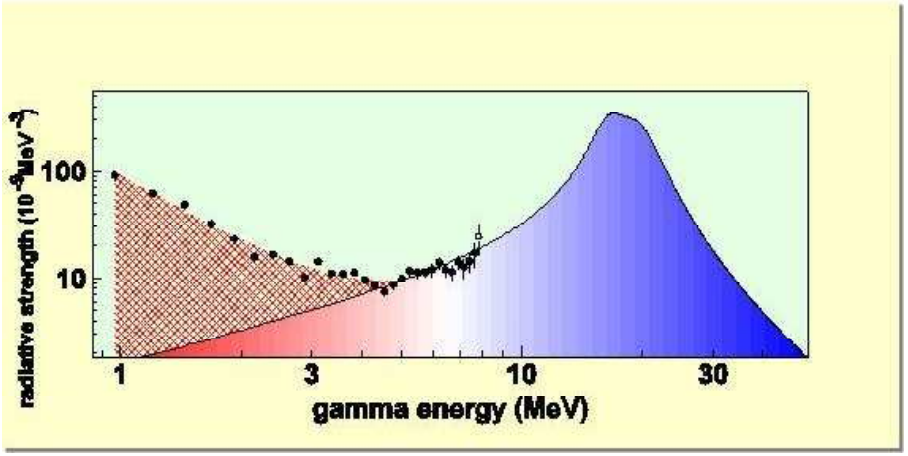

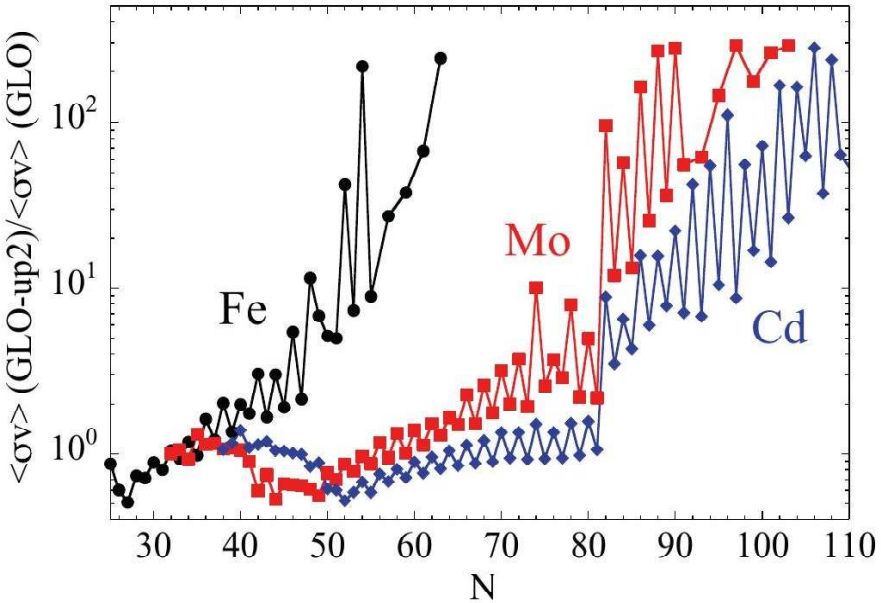

"The nucleus goes red."
Unexpected upbend of dipole strength toward low energy observed in Fe, Mo, Cd isotopes.

Courtesy of M. Guttormsen.

Ratios of Maxwellian-averaged (n,γ) reaction rates at $T = 10^9$ K for isotopic chains up to the neutron drip line using strength functions with and without low-energy upbend of dipole strength.

A.C. Larsen, S. Goriely, PRC 82, 014318 (2010)

$\Rightarrow$ Big influence of low-energy strength on neutron-capture rates of very neutron-rich nuclei in the astrophysical r-process.

Gamma-ray strength functions

- Gamma-ray strength functions describe average electromagnetic transition strengths in the quasicontinuum of nuclear states at high excitation energy:

$$f_{fiL}(E_\gamma) = \overline{\Gamma_{fiL}}\ \rho(E_i, J_i)\ /\ E_\gamma^{2L+1} \qquad E_\gamma = E_i - E_f \qquad J_i = 0,\ ...,\ J_{\mathrm{max}}$$

- Photoabsorption:

$$f_L = \sigma_\gamma\ /\ [(2J_i{+}1)/(2J_0{+}1)\ (\pi\hbar c)^2\ E_\gamma^{2L-1}] \qquad E_\gamma = E_i \qquad J_i = 1,\ (2)$$

- Brink-Axel hypothesis:
  The strength function does not depend on the excitation energy.
  The strength function for excitation is identical with the one for deexcitation.

The bremsstrahlung facility at the electron accelerator ELBE

Accelerator parameters:

- Maximum electron energy: $\approx$ 18 MeV
- Maximum average current: $\approx$ 0.8 mA
- Micro-pulse rate: 13 MHz
- Micro-pulse length: $\approx$ 5 ps

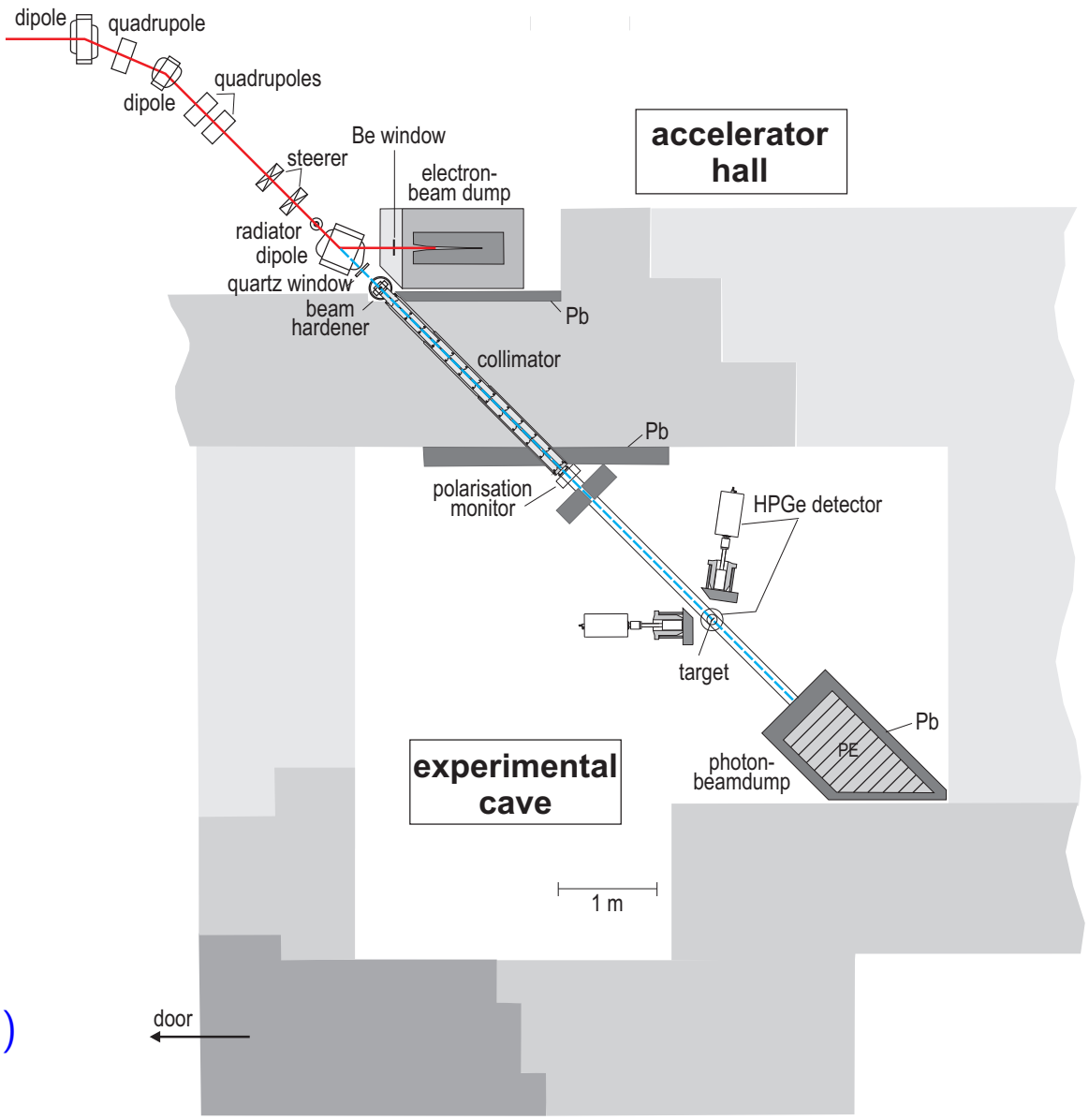

R.S. et al., NIM A 555, 211 (2005)

Detector setup at γELBE

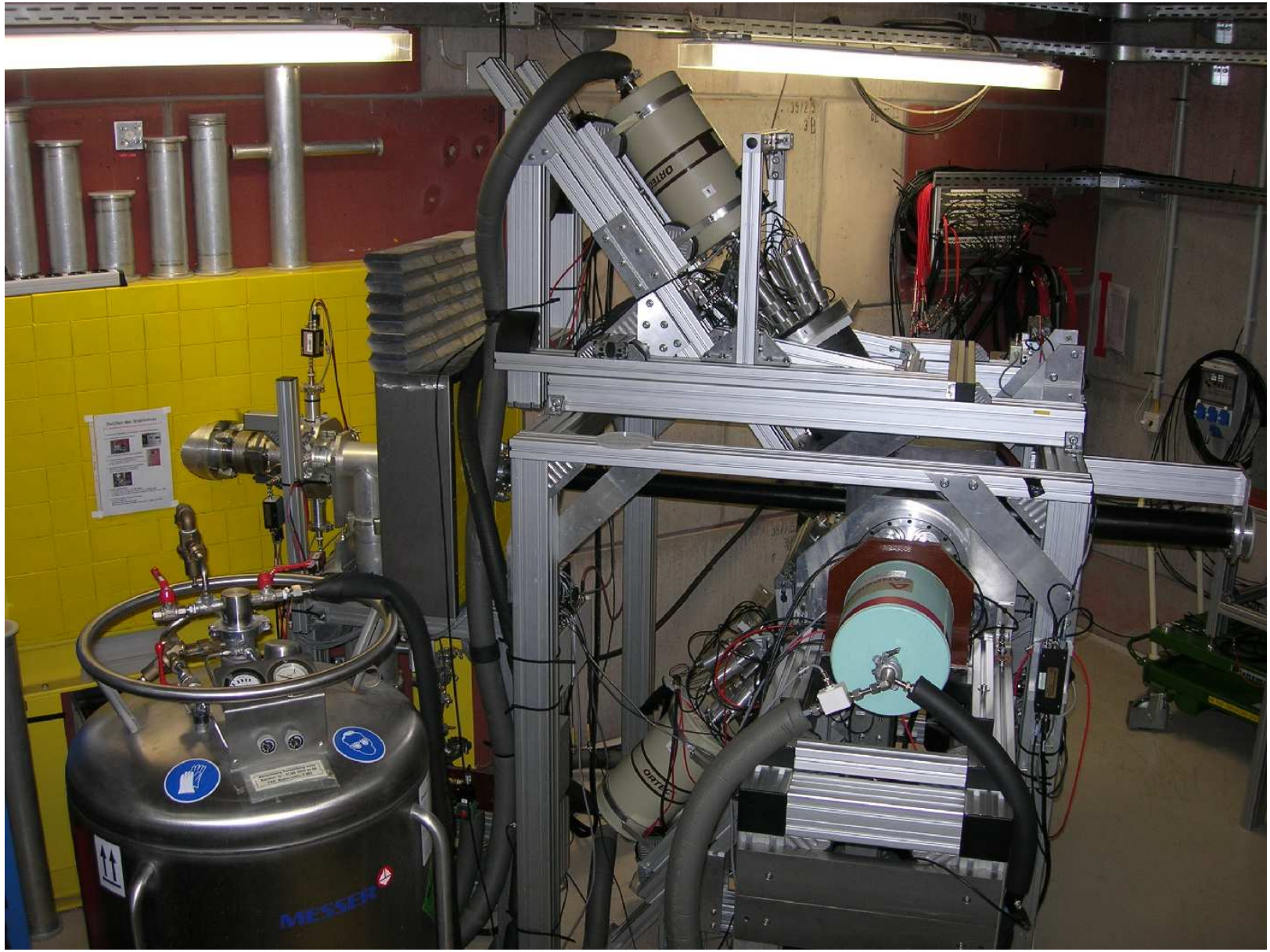

High Intensity Gamma-ray Source (HIGS) at TUNL

- Highest intensity (γ-rays/s/keV) γ-ray beam in the world
- Produces γ-rays by Compton backscattering inside the optical cavity of a storage-ring FEL
- Produces both linearly and circularly polarized beams

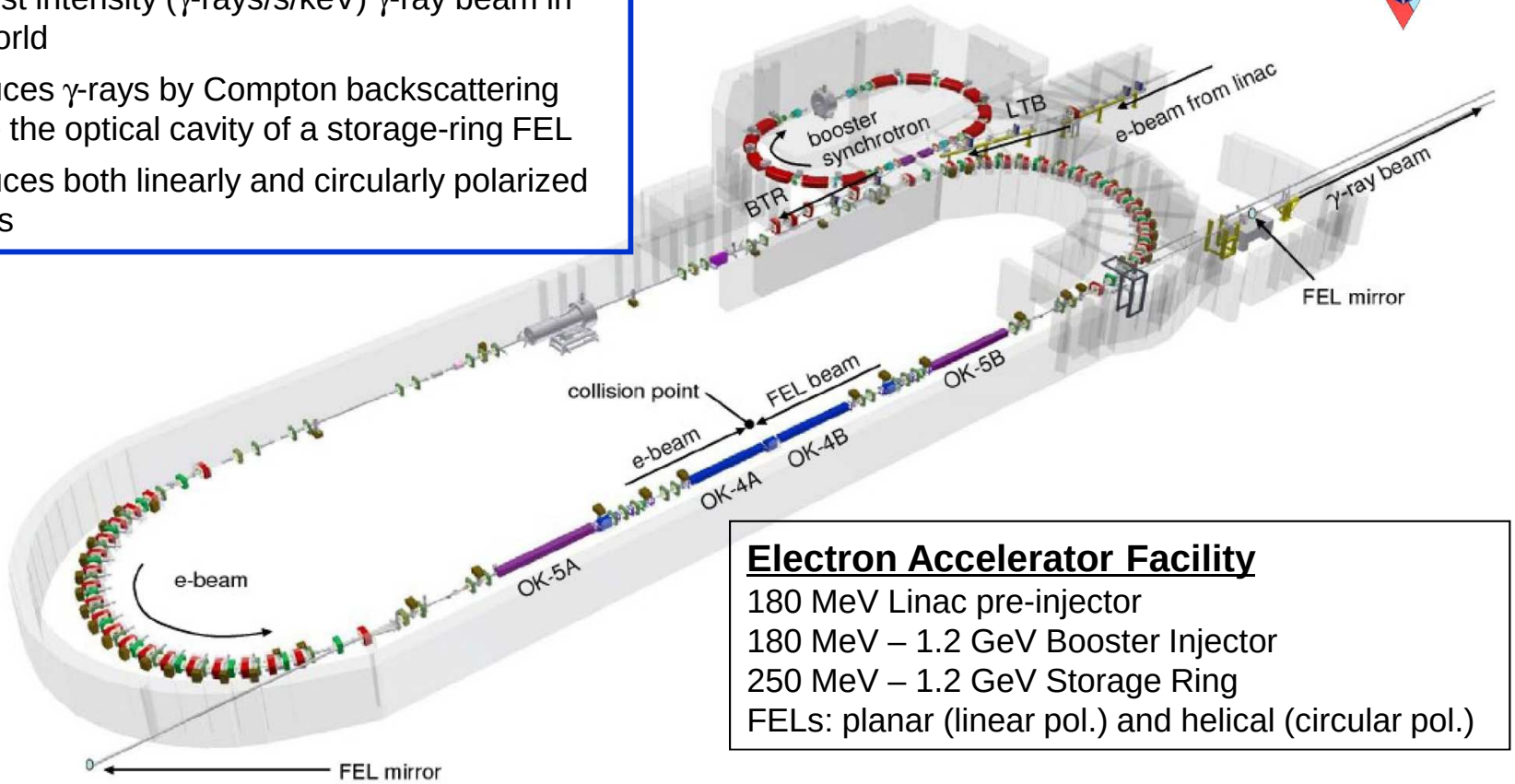

Electron Accelerator Facility
180 MeV Linac pre-injector
180 MeV – 1.2 GeV Booster Injector
250 MeV – 1.2 GeV Storage Ring
FELs: planar (linear pol.) and helical (circular pol.)

γ-ray beam parameters	Values
Energy	1 – 100 MeV
Linear & circular polarization	> 95%
Intensity with 5% $\Delta E_\gamma/E_\gamma$	> 10^7 γ/s

For more details see:
http://www.tunl.duke.edu/higs/

Courtesy of C. Howell (TUNL)

Flux spectra at γELBE and HIγS

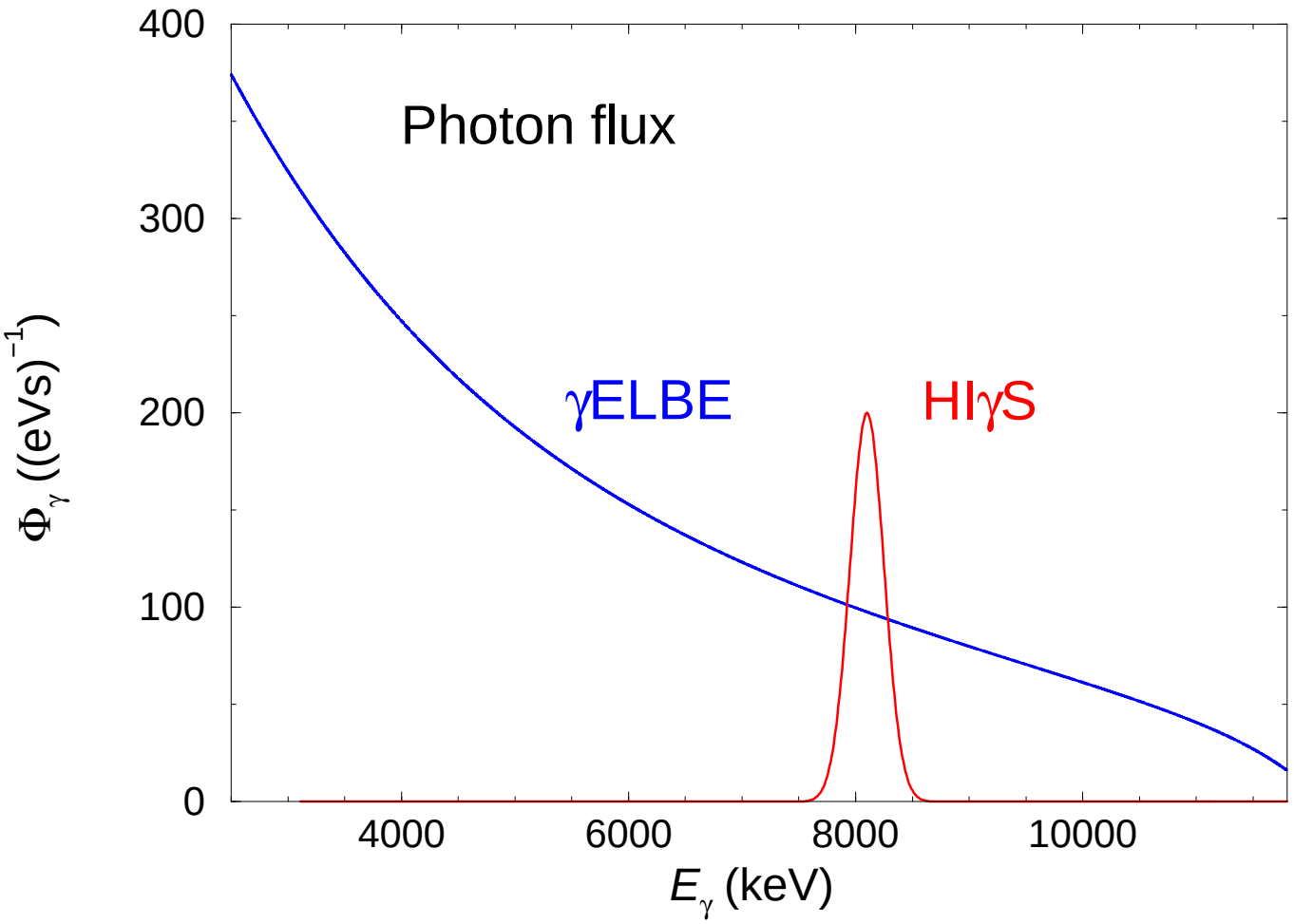

Measurements at γELBE and HIγS

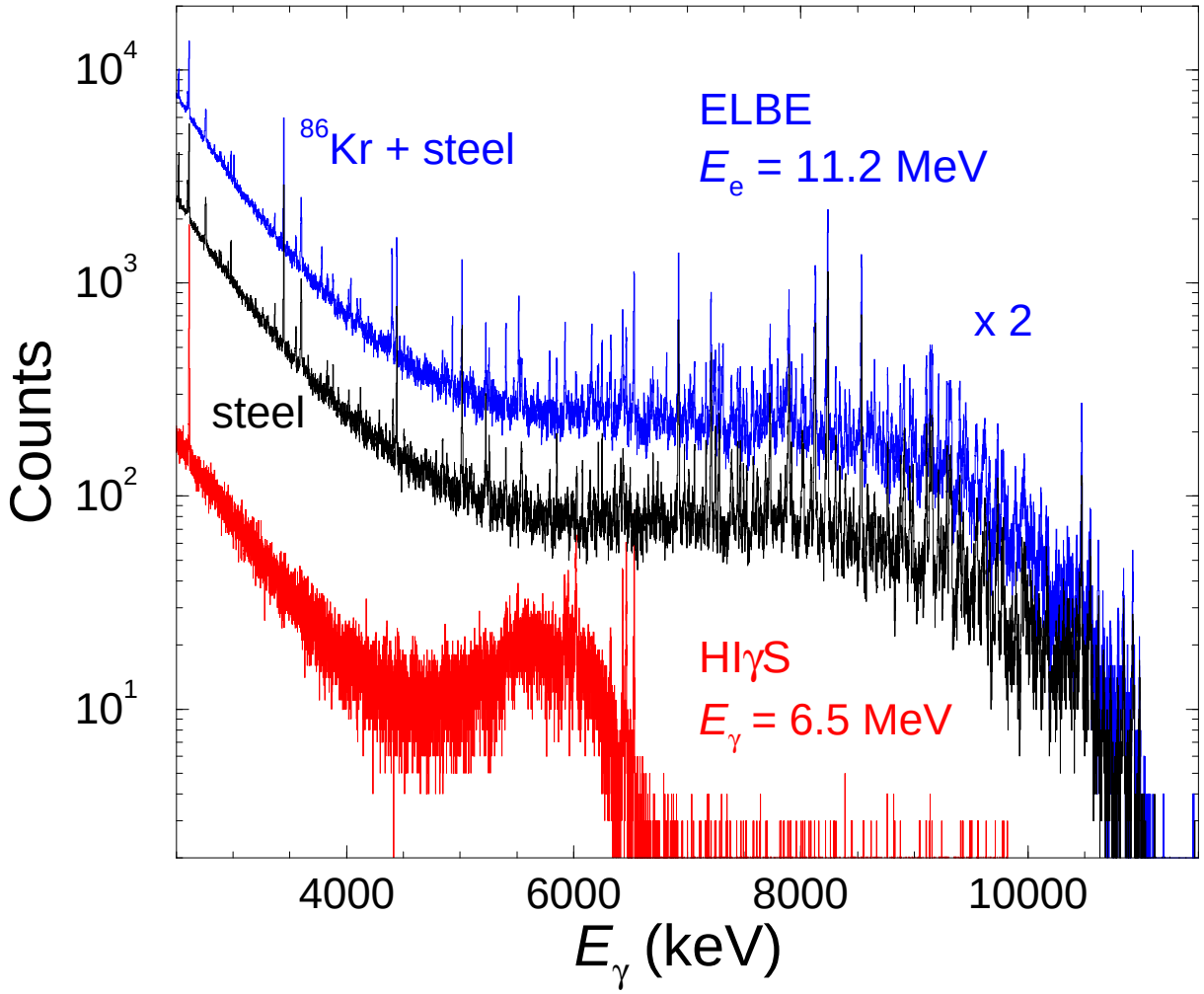

Identification of transitions in ^{86}Kr by comparison of spectra measured with the filled and with the empty steel container.

R.S. et al., PRC 87, 024306 (2013)

Unresolved strength in the quasicontinuum

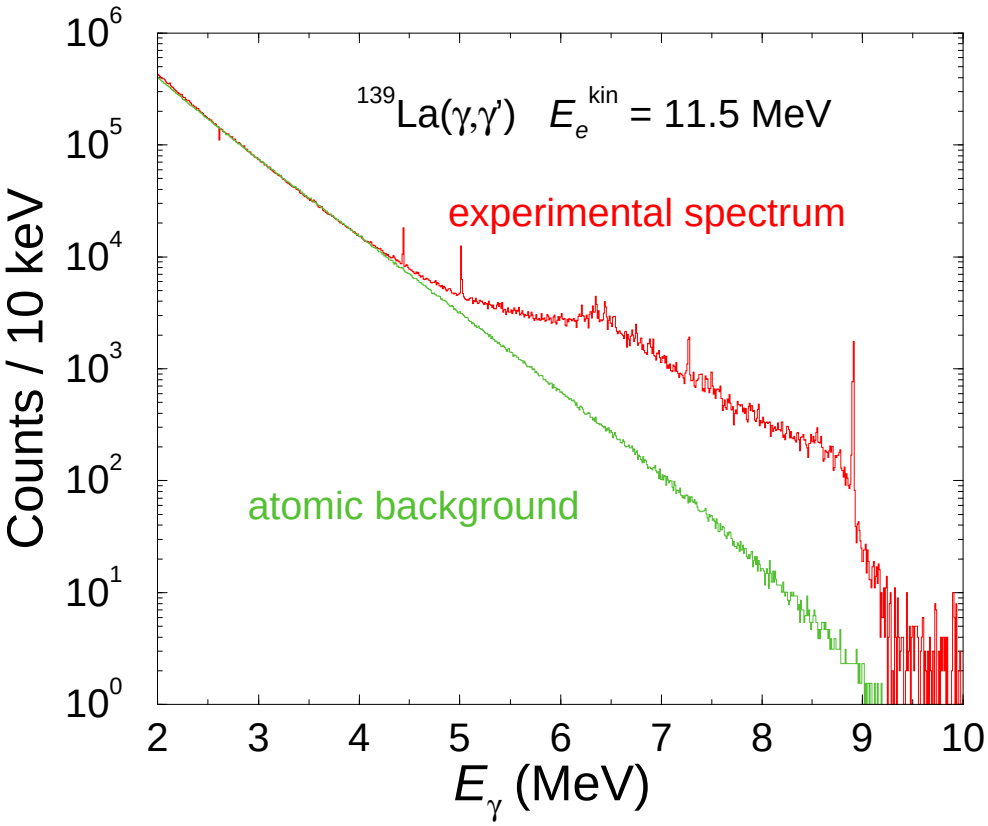

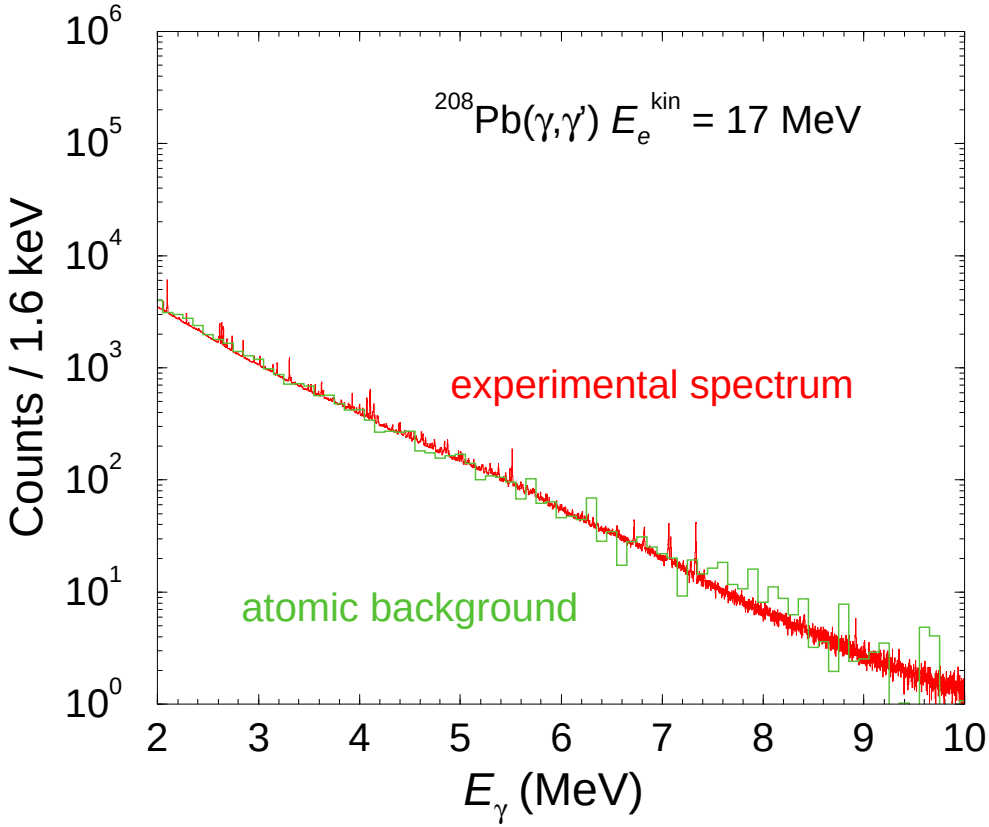

Experimental spectra (corrected for room background, detector response and efficiency) and simulated spectra of atomic background.

^{139}La data: A. Makinaga et al., PRC 82, 024314 (2010).
^{208}Pb data: R.S. et al., PRC 81, 054315 (2010).

Photon scattering - feeding and branching

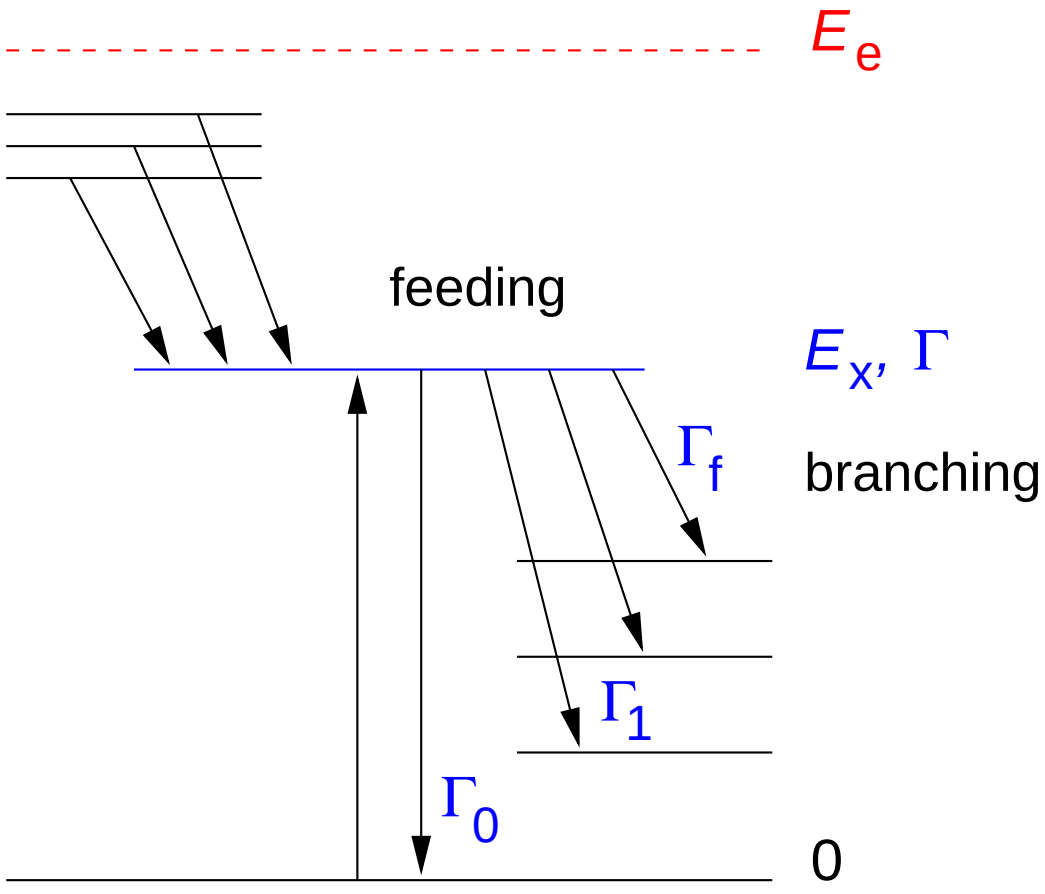

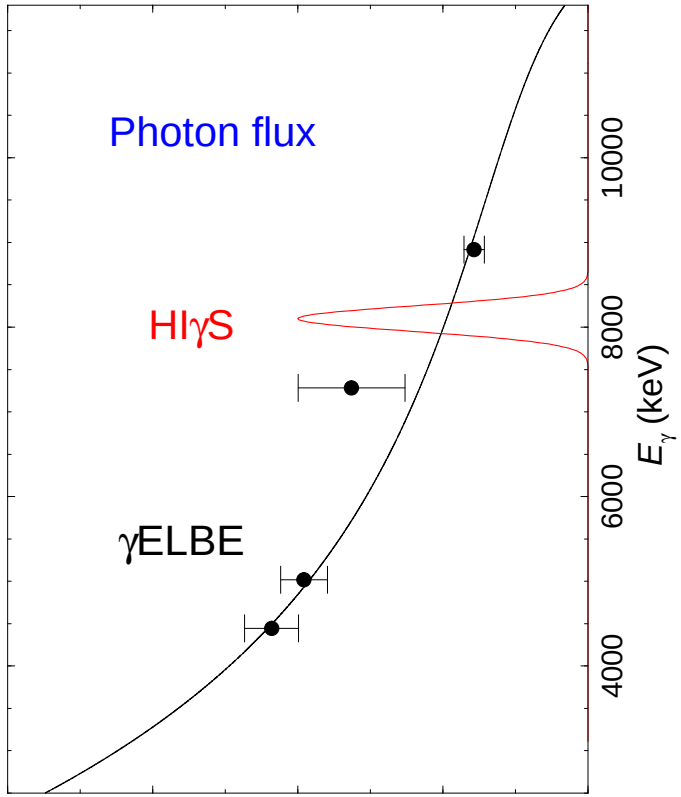

Simulations of γ-ray cascades

Monte Carlo:
G. Rusev et al., PRC 77, 064321 (2008)
Code γDEX:
G. Schramm et al., PRC 85, 014311 (2012)
R. Massarczyk et al., PRC 86, 014319 (2012); PRC 87, 044306 (2013)

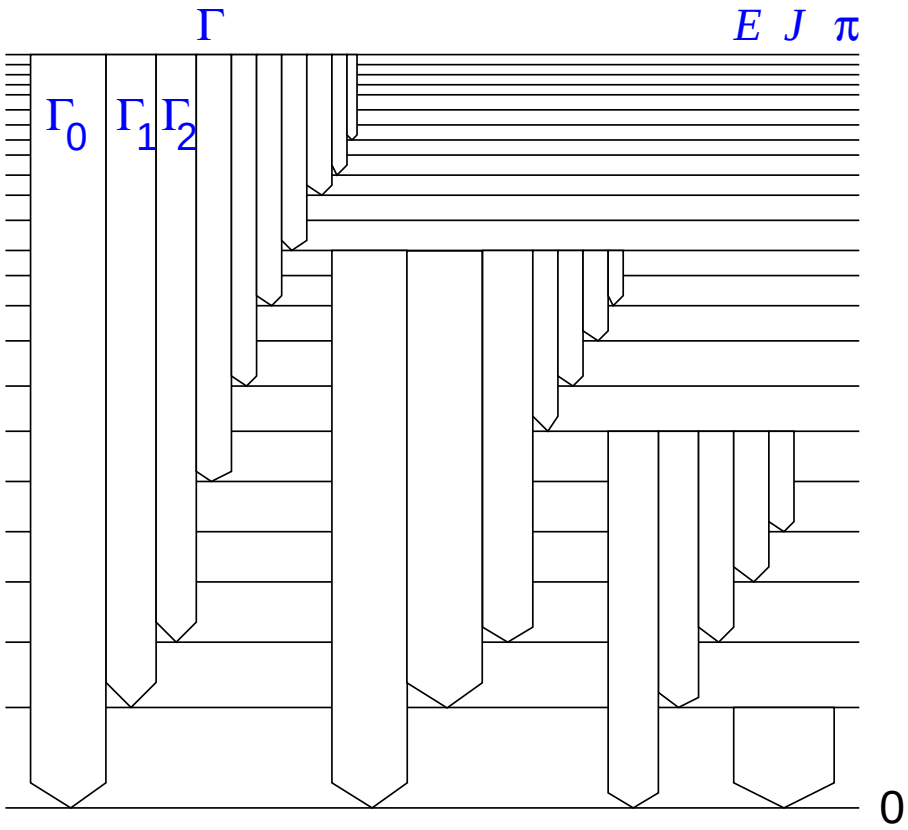

⇒ Level scheme of $J = |J_0 \pm 1, ..., 5|$ states in 10 keV energy bins constructed by using:
- Constant-Temperature Model with level-density parameters from T. v. Egidy, D. Bucurescu, PRC 80, 054310 (2009).
- Parity distribution of level densities according to S. I. Al-Quraishi et al., PRC 67, 015803 (2003).
- Wigner level-spacing distributions.

⇒ Partial decay widths calculated by using:
- Photon strength functions approximated by Lorentz curves (www-nds.iaea.org/RIPL-2).
- Porter-Thomas distributions of decay widths.

⇒ Subtraction of feeding intensities and correction of intensities of g.s. transitions with calculated branching ratios Γ_0/Γ.

⇒ Determination of the absorption cross section.

Simulations of γ-ray cascades

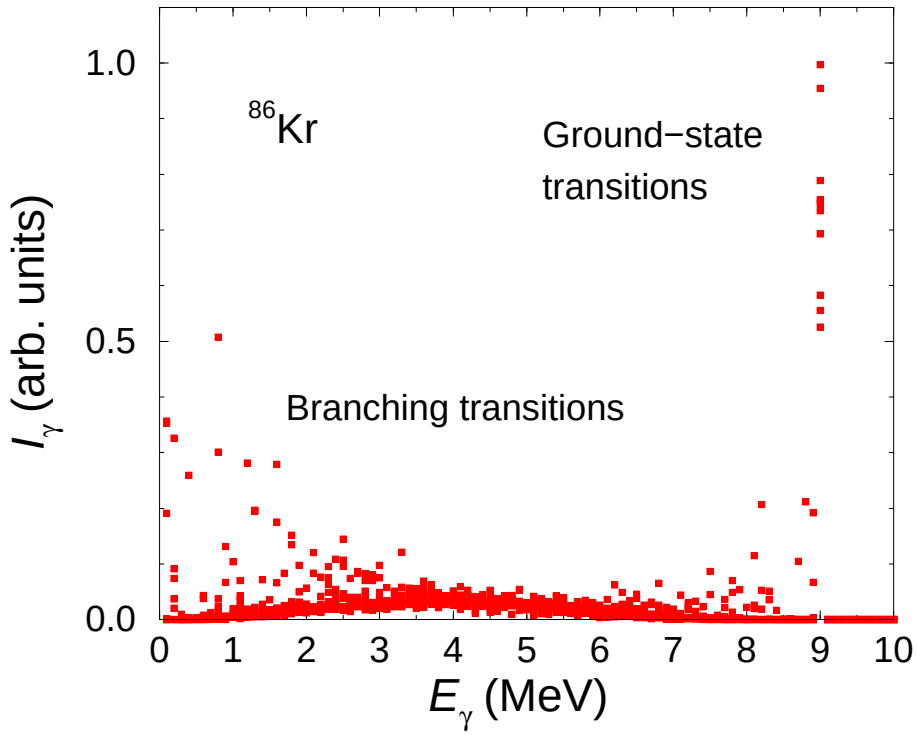

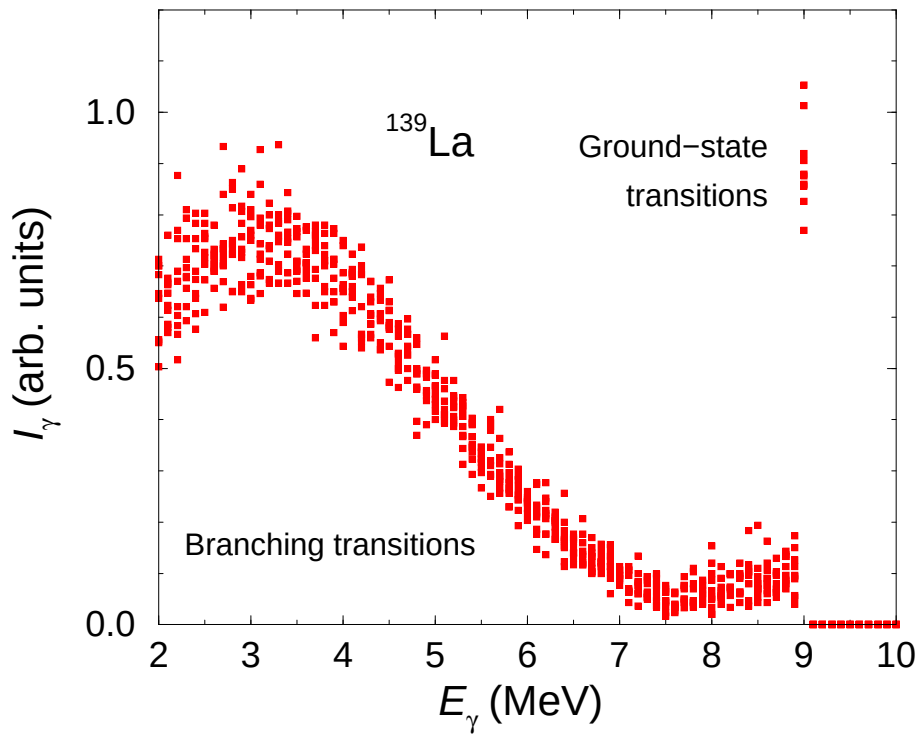

Simulated intensity distribution of transitions depopulating levels in a 100 keV bin around 9 MeV.

$\Rightarrow$ Subtraction of intensities of branching transitions.

^{86}Kr data: R.S. et al., PRC 87, 024306 (2013).

^{139}La data: A. Makinaga et al., PRC 82, 024314 (2010).

Branching ratios in ^{136}Ba from measurements at HIγS

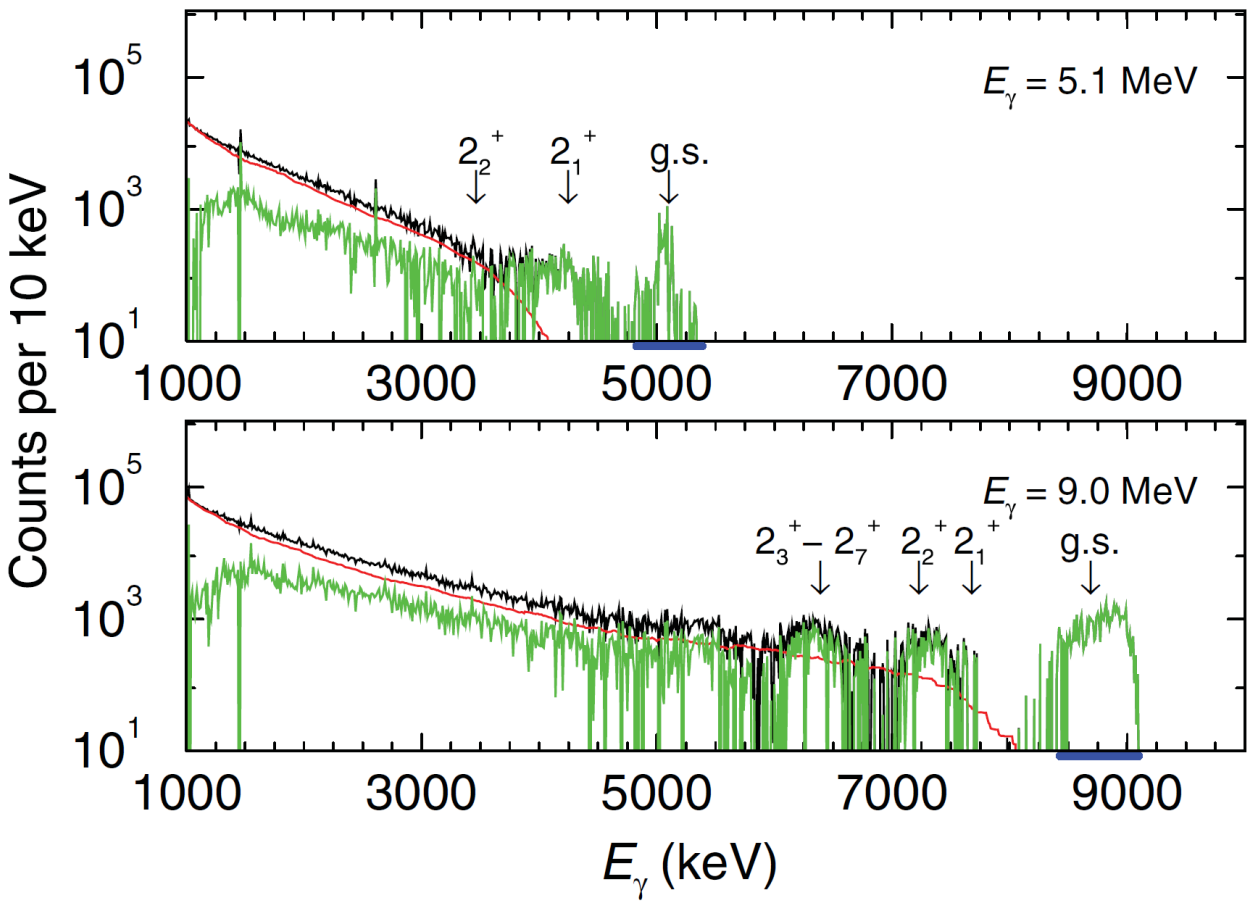

Response-corrected spectra.

Simulated spectra of γ rays scattered by atomic processes.

Subtracted spectra contain bunches of transitions to the ground state and to excited states.

$\Rightarrow$ Intensities of branching transitions to low-lying 2^+ states deduced.

R. Massarczyk et al., PRC 86, 014319 (2012).

Test of simulated branching ratios - measurements at HIγS

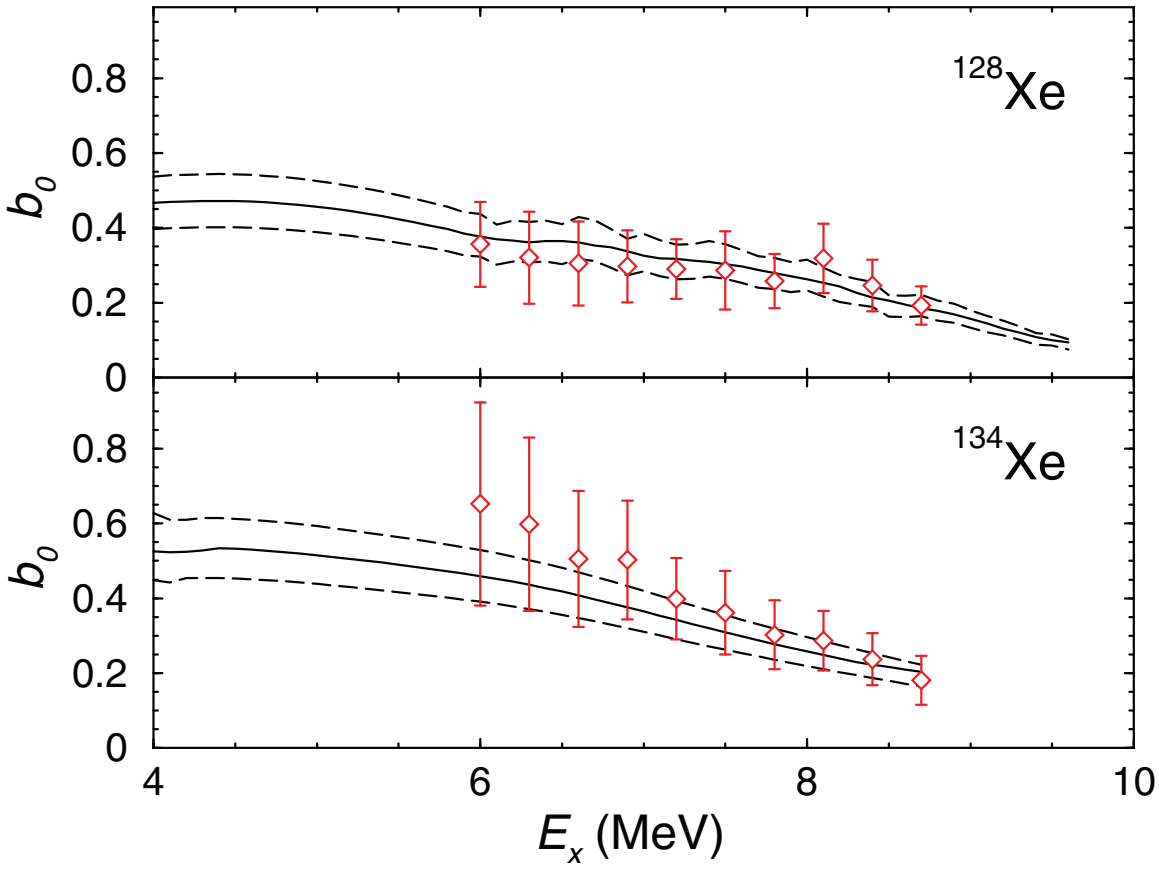

Red diamonds:

Branching ratios deduced from measurements with monoenergetic γ rays at HIγS ($\Delta E \approx 200$ keV).

Black lines:

Average branching ratios (solid) $b_0 = \Gamma_0/\Gamma$ versus the excitation energy as obtained from simulations of γ-ray cascades and their uncertainties (dashed).

R. Massarczyk et al., PRC 90, 054310 (2014).

Absorption cross section in ^{86}Kr

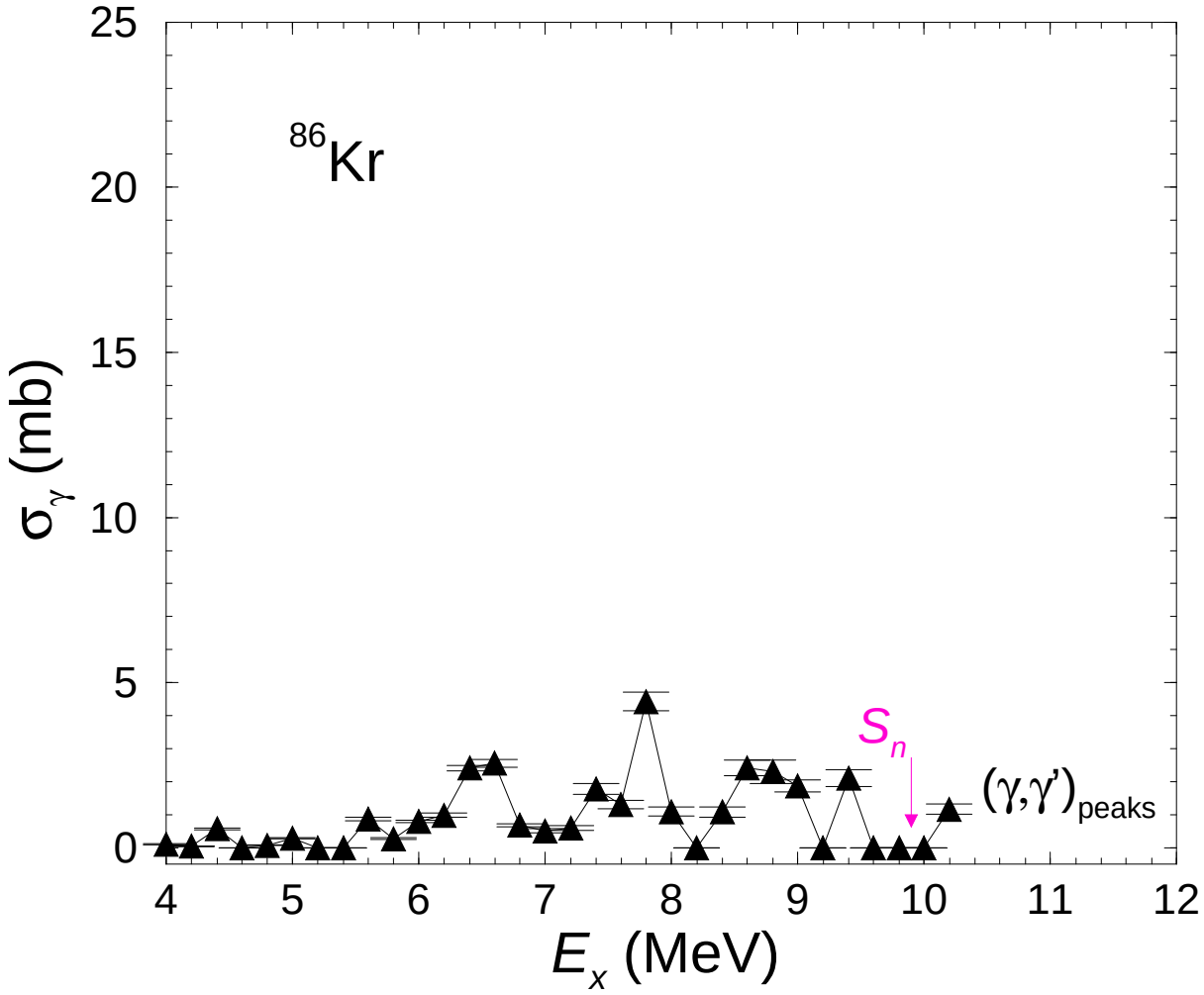

(γ, γ') data from γELBE

R.S. et al., PRC 87, 024306 (2013)

Absorption cross section in ^{86}Kr

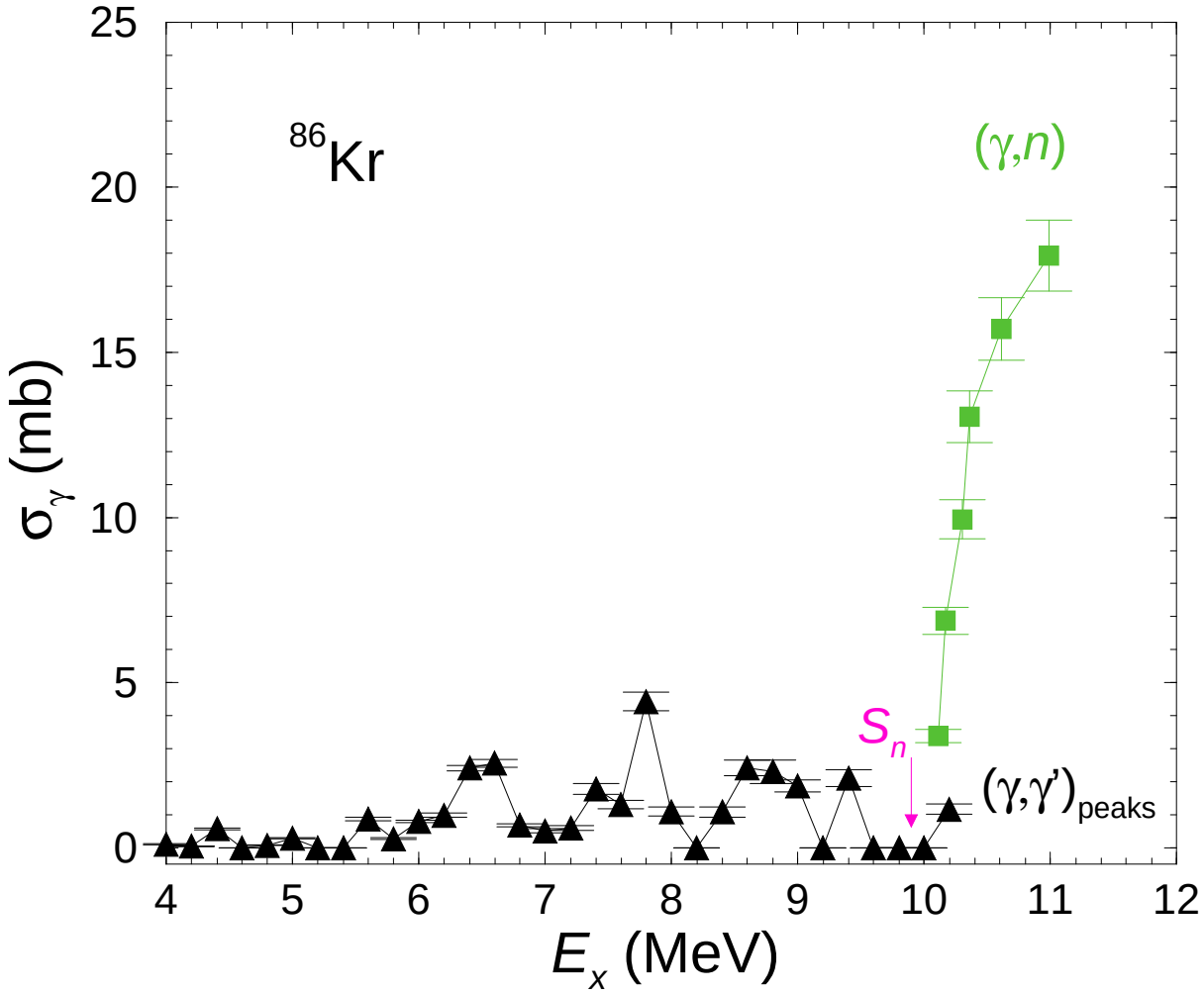

(γ, γ') data from γELBE

R.S. et al., PRC 87, 024306 (2013)

(γ, n) data from HIγS

R. Raut et al., PRL 111, 112501 (2013)

Absorption cross section in ^{86}Kr

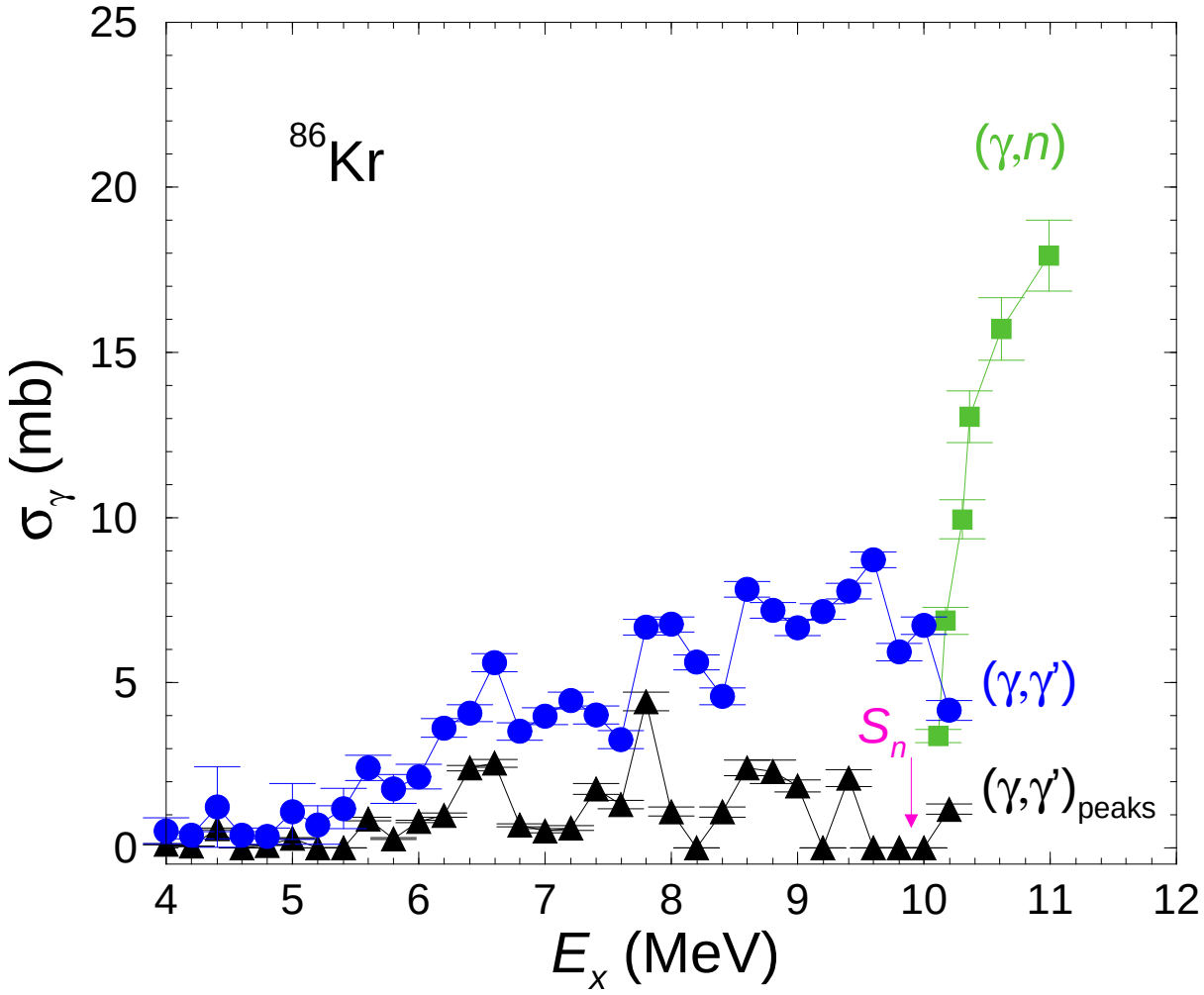

(γ, γ') data from γELBE

R.S. et al., PRC 87, 024306 (2013)

(γ, n) data from HIγS

R. Raut et al., PRL 111, 112501 (2013)

Absorption cross section in ^{86}Kr

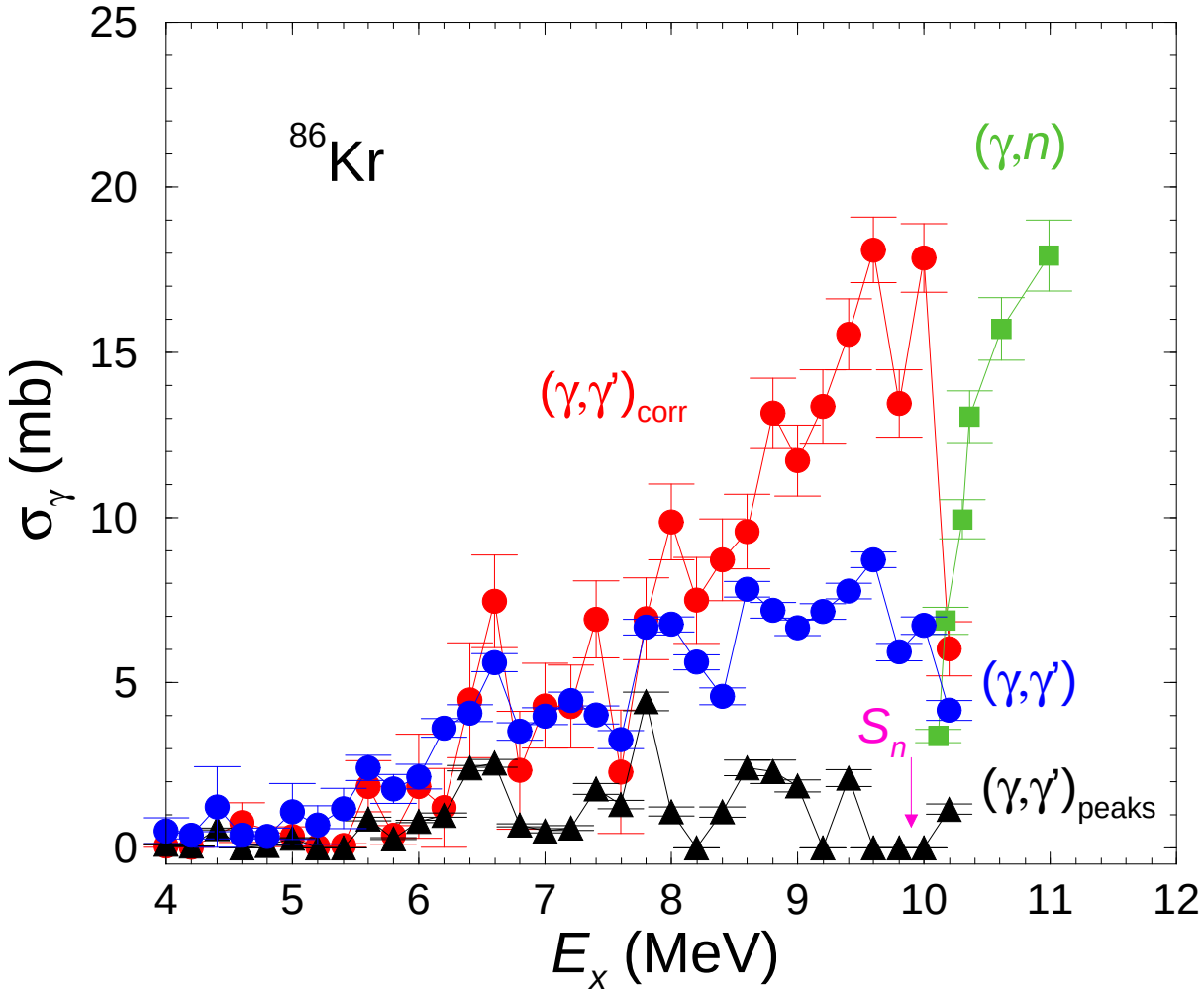

(γ, γ') data from γELBE

R.S. et al., PRC 87, 024306 (2013)

(γ, n) data from HIγS

R. Raut et al., PRL 111, 112501 (2013)

Absorption cross section in ^{86}Kr

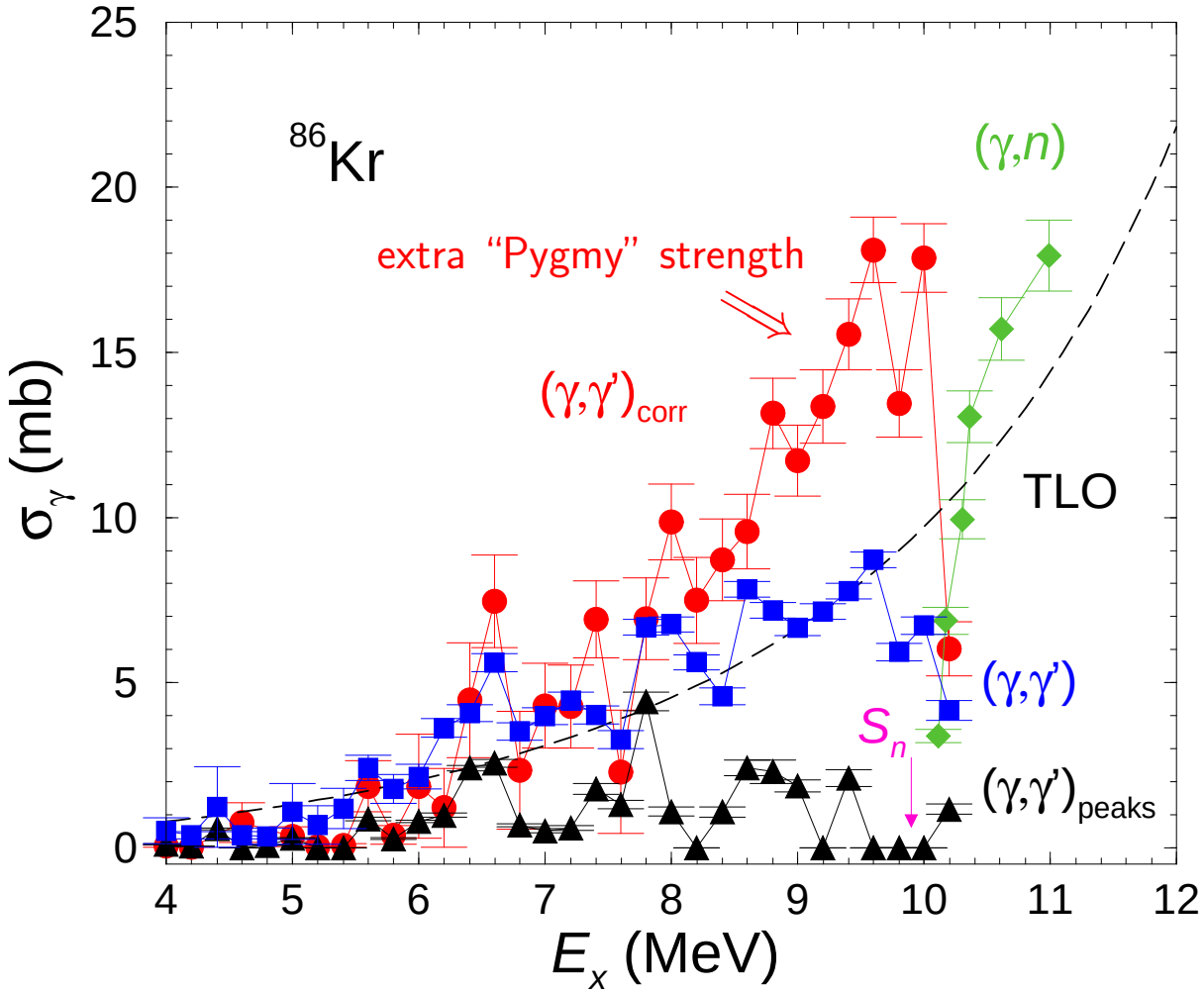

(γ, γ') data from γELBE

R.S. et al., PRC 87, 024306 (2013)

(γ, n) data from HIγS

R. Raut et al., PRL 111, 112501 (2013)

TLO

A.R. Junghans et al.,

PLB 670, 200 (2008)

Influence of nuclear properties on the pygmy strength

Summed dipole strength in stable even-mass xenon isotopes:

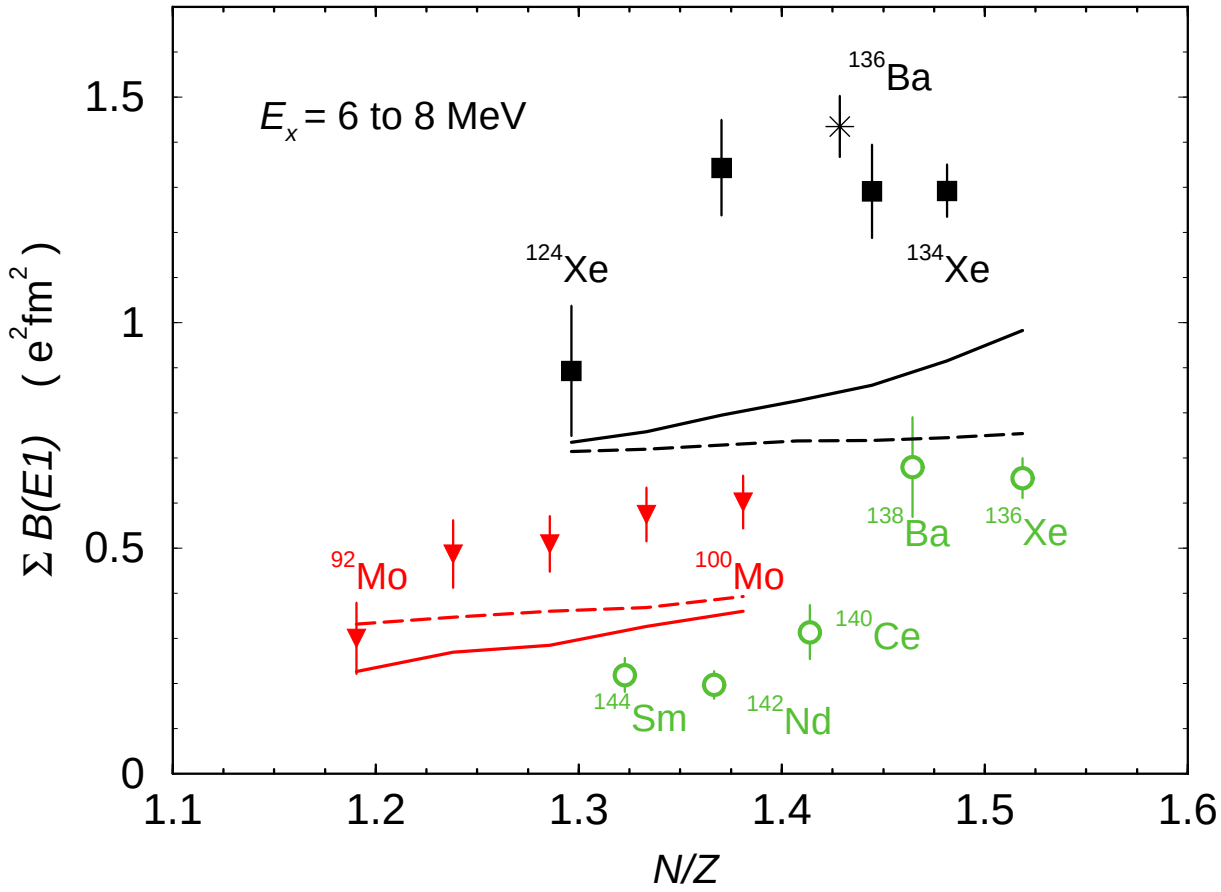

neutron excess

Solid lines:
QRPA calculations
in a deformed basis

Dashed lines:
TLO with deformation

Summed E1 strength increases
with the neutron excess

R. Massarczyk et al.,
PRL 112, 072501 (2014)

Influence of nuclear properties on the pygmy strength

Summed dipole strength in stable even-mass xenon isotopes:

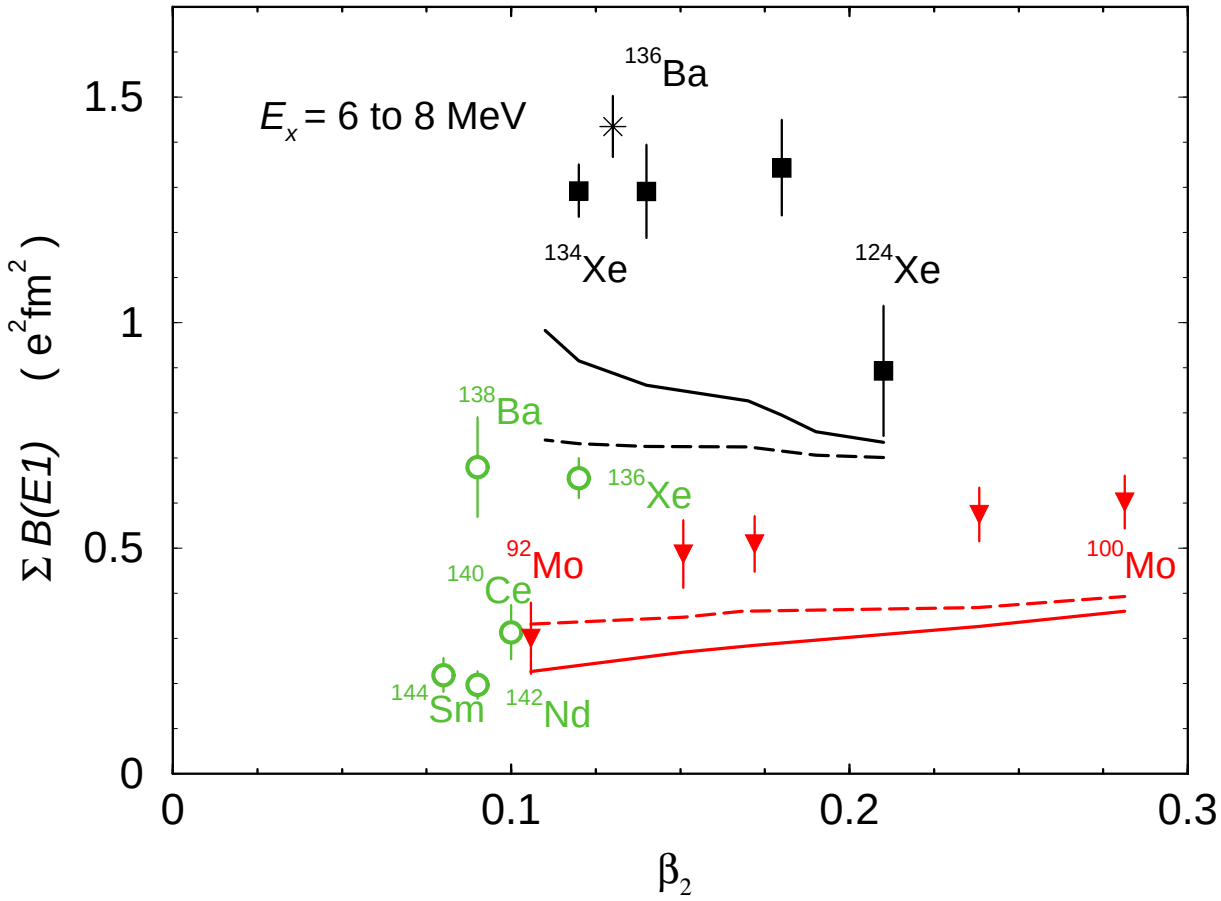

quadrupole deformation

Solid lines:
QRPA calculations
in a deformed basis

Dashed lines:
TLO with deformation

Minor influence of the deformation
on the summed E1 strength

R. Massarczyk et al.,
PRL 112, 072501 (2014)

E1 strength in the PDR region and M1 strength in the spin-flip region

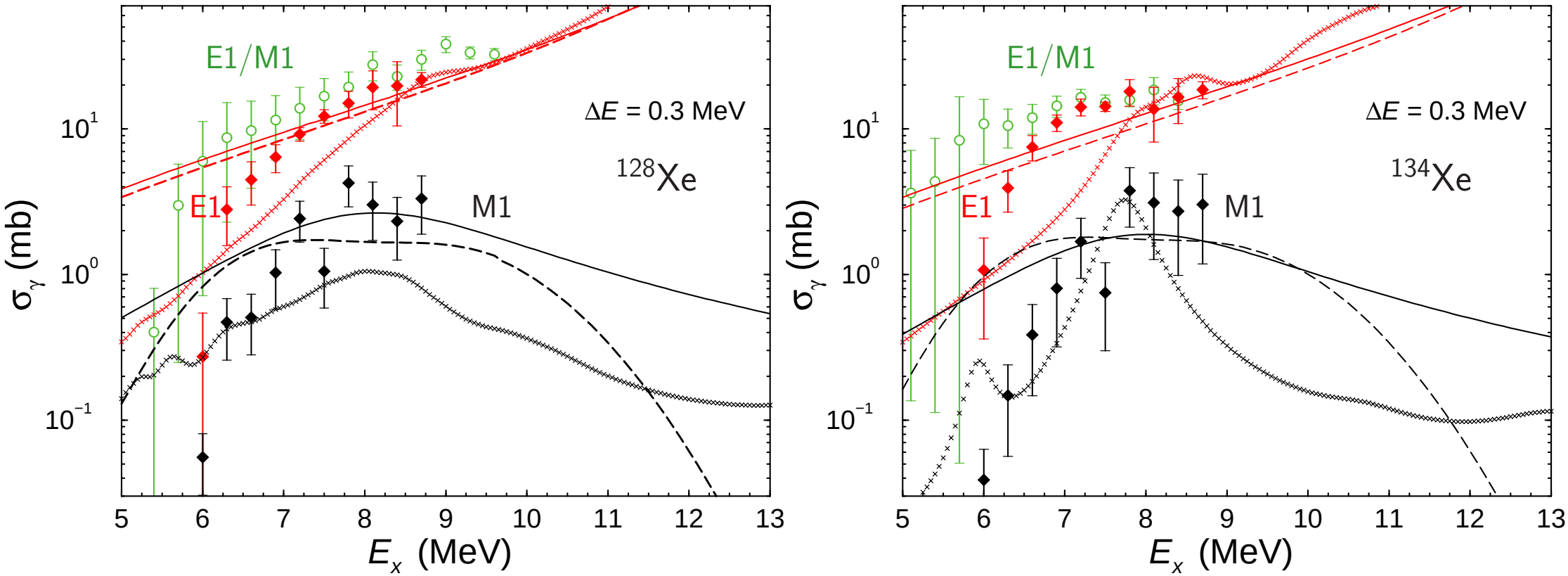

Solid lines: RIPL. *Dashed lines:* E. Grosse et al., EPJA 53, 225 (2017). *Crosses:* deformed QRPA.

E1/M1: strength from experiments at γELBE.
E1 and M1: strengths from experiments at HIγS. Intensities include the quasicontinuum.

R. Massarczyk et al., PRC 90, 054310 (2014)

Absorption cross section of ^{74}Ge

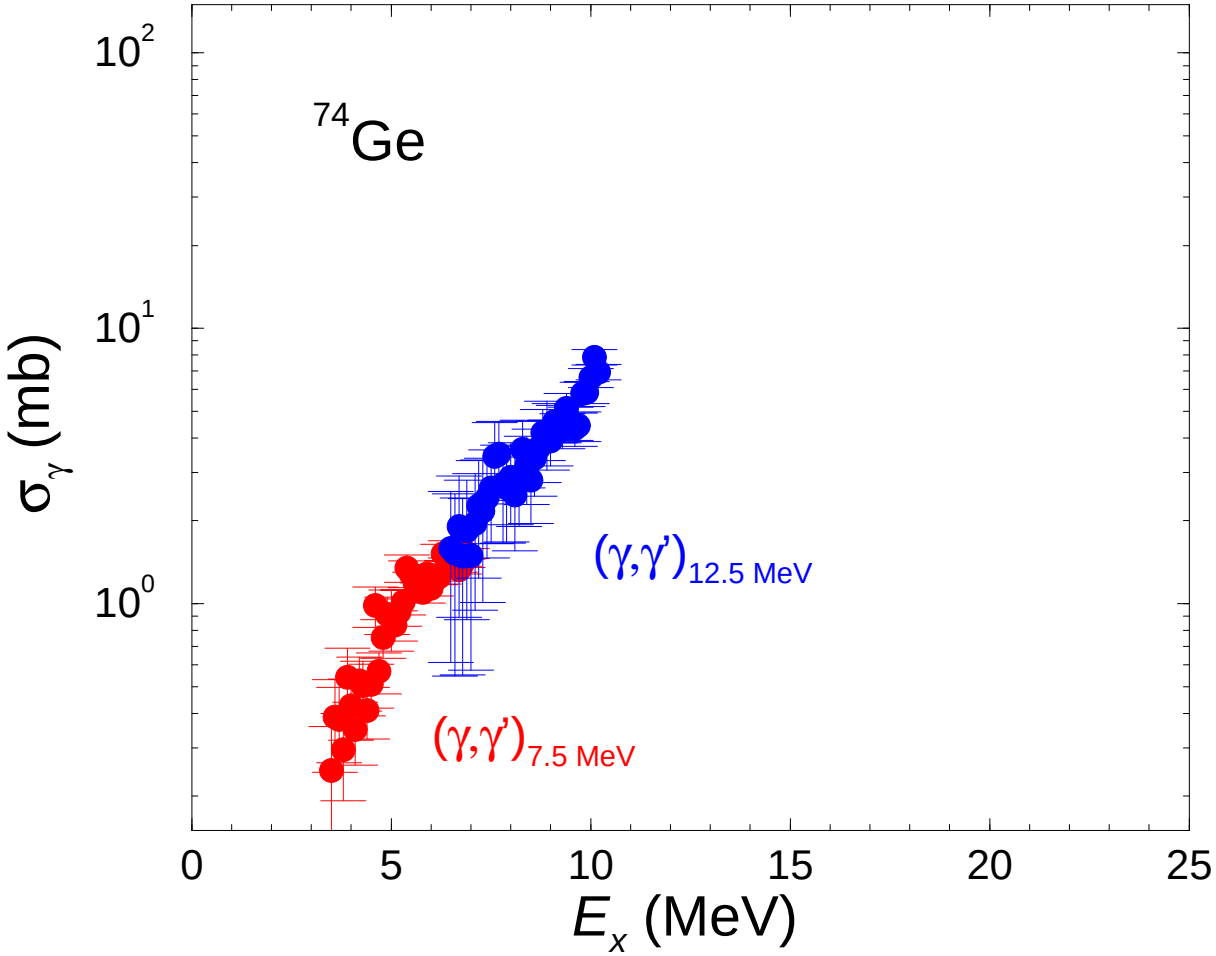

(γ, γ') data (HZDR):

R. Massarczyk et al.

PRC 92, 044309 (2015)

Absorption cross section of ^{74}Ge

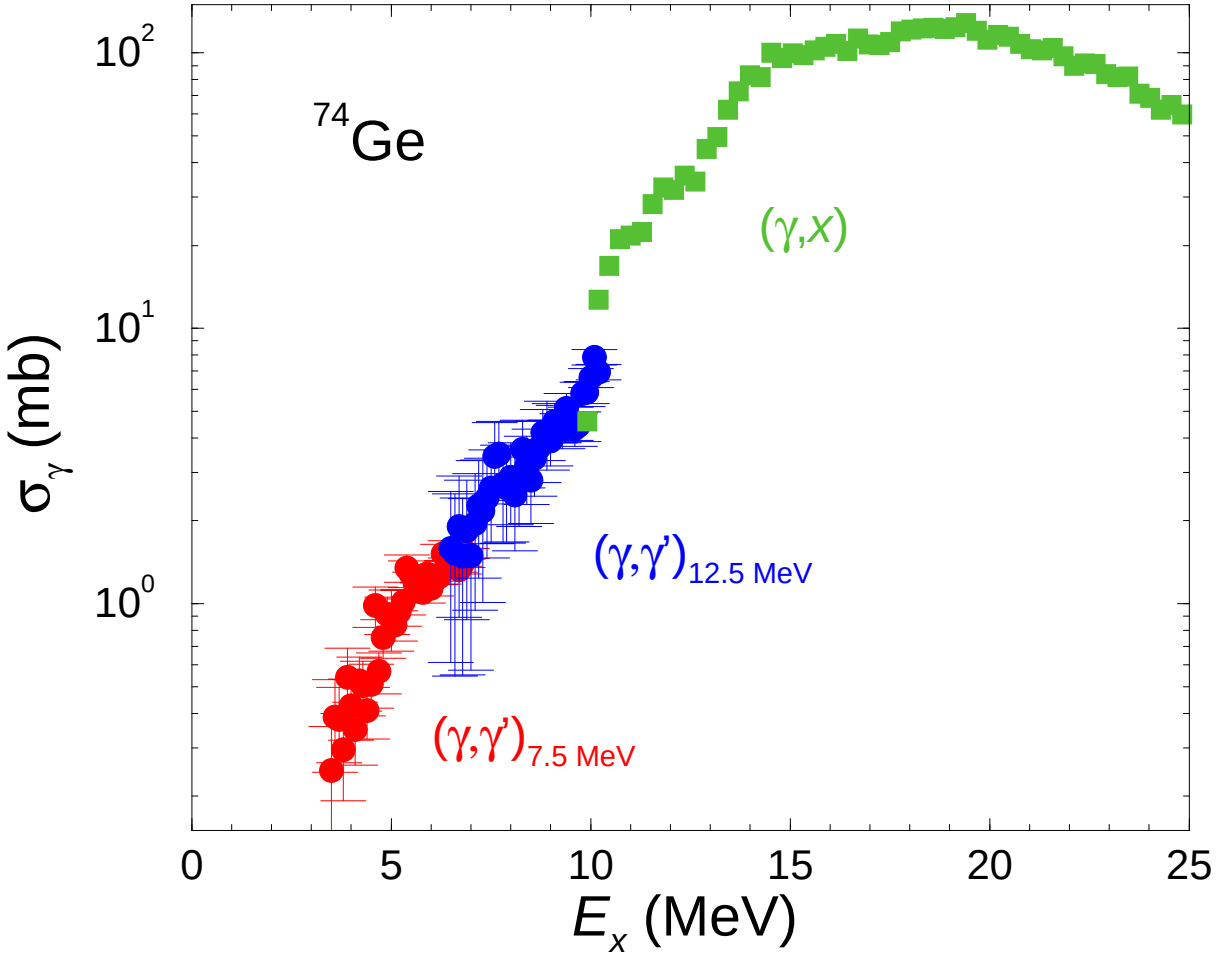

(γ, γ') data (HZDR):

R. Massarczyk et al.

PRC 92, 044309 (2015)

(γ,x) data:

P. Carlos et al.,

NPA 258, 365 (1976)

Dipole strength functions in ^{74}Ge

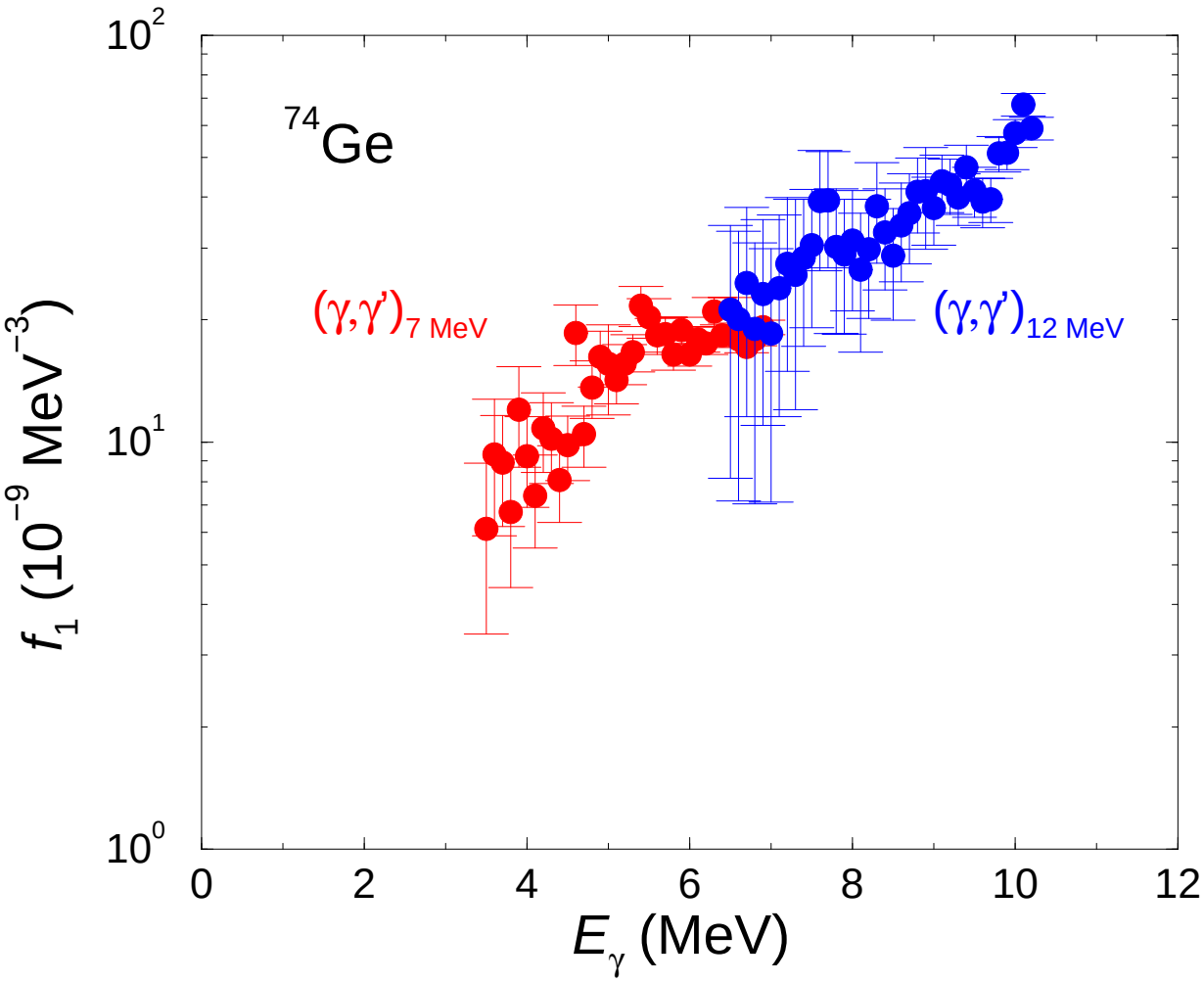

(γ, γ') data (HZDR):

R. Massarczyk et al.

PRC 92, 044309 (2015)

Dipole strength functions in ^{74}Ge

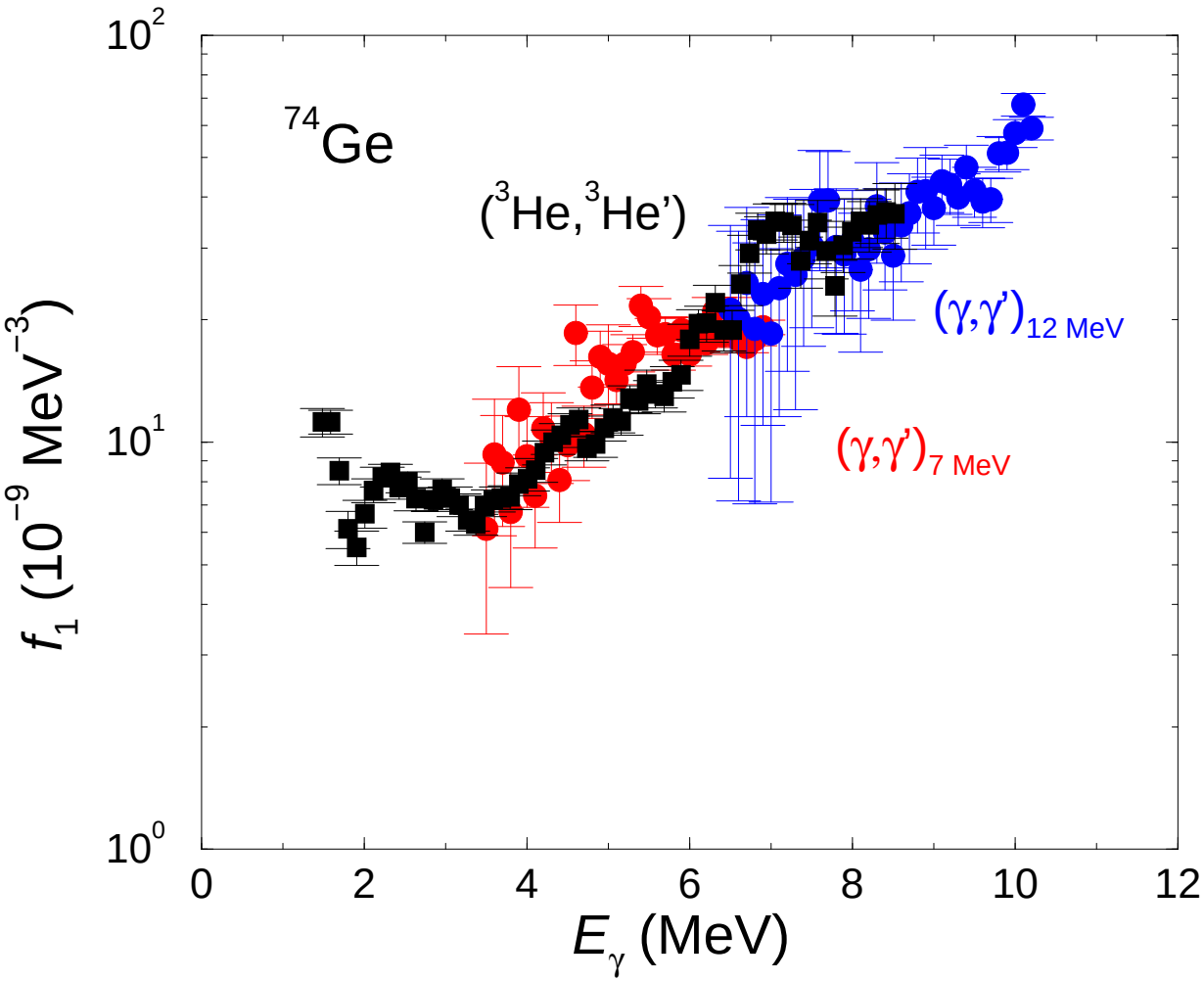

(γ, γ') data (HZDR):

R. Massarczyk et al.

PRC 92, 044309 (2015)

(^{3}He,^{3}He') data (OCL):

T. Renstrøm et al.

PRC 93, 064302 (2016)

Dipole strength functions in ^{74}Ge

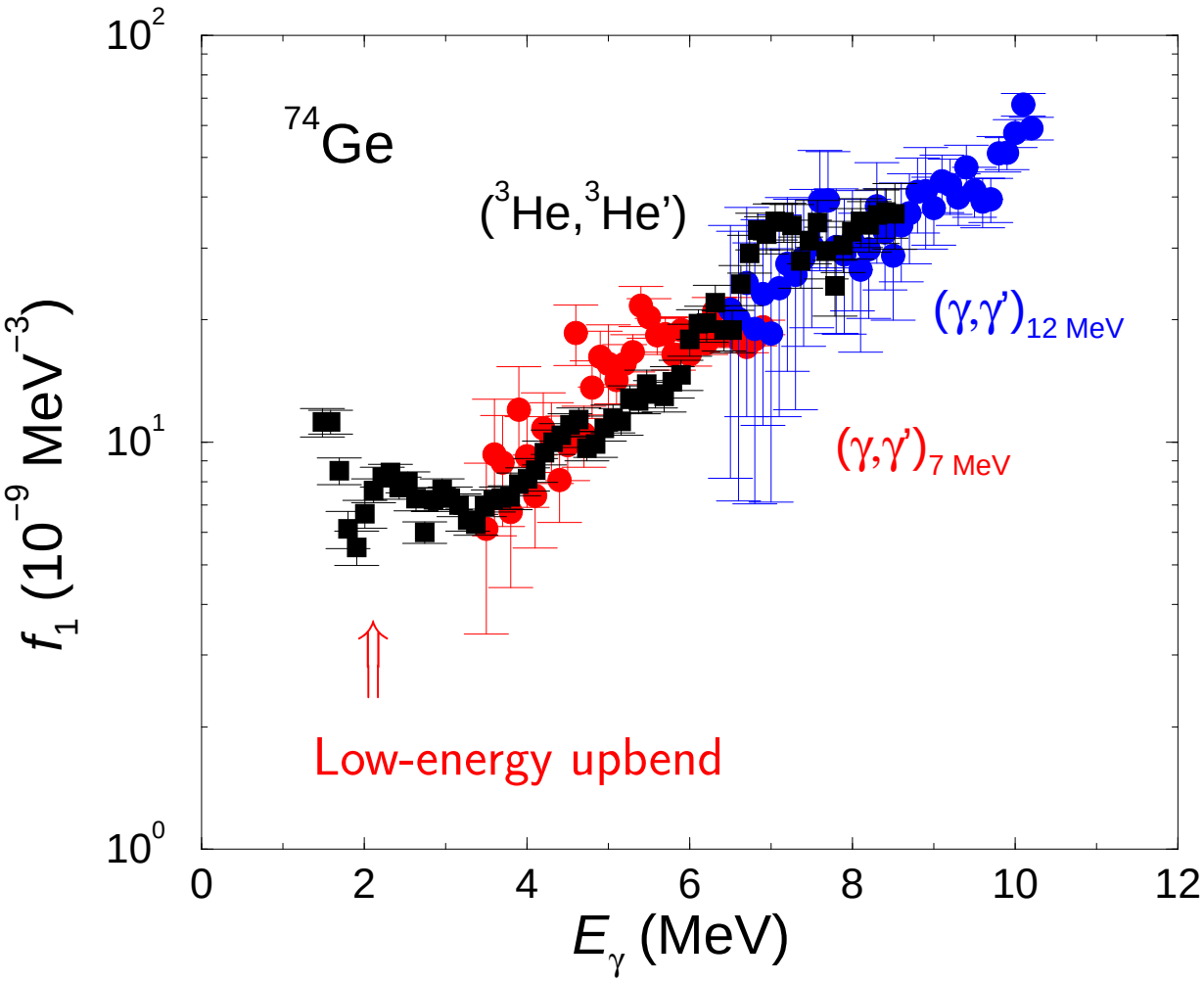

(γ, γ') data (HZDR):

R. Massarczyk et al.

PRC 92, 044309 (2015)

(^{3}He,^{3}He') data (OCL):

T. Renstrøm et al.

PRC 93, 064302 (2016)

What is the origin of the upbend?

Calculations of M1 strength functions

Can model calculations describe the low-energy upbend of dipole strength?

Shell-model calculations:

- 40 levels of each spin from 0 to 10 for each parity.
- All possible transitions between these 440 states - about 24000 M1 transitions.
- Average B(M1) values in bins of E_γ.
- M1 strength function.

Codes:

- NuShellX@MSU
  B.A. Brown and W.D.M. Rae, Nucl. Data Sheets 120, 115 (2014).
- RITSSCHIL
  D. Zwarts, Comput. Phys. Commun. 38, 365 (1985).

Shell-model calculations of M1 strength functions

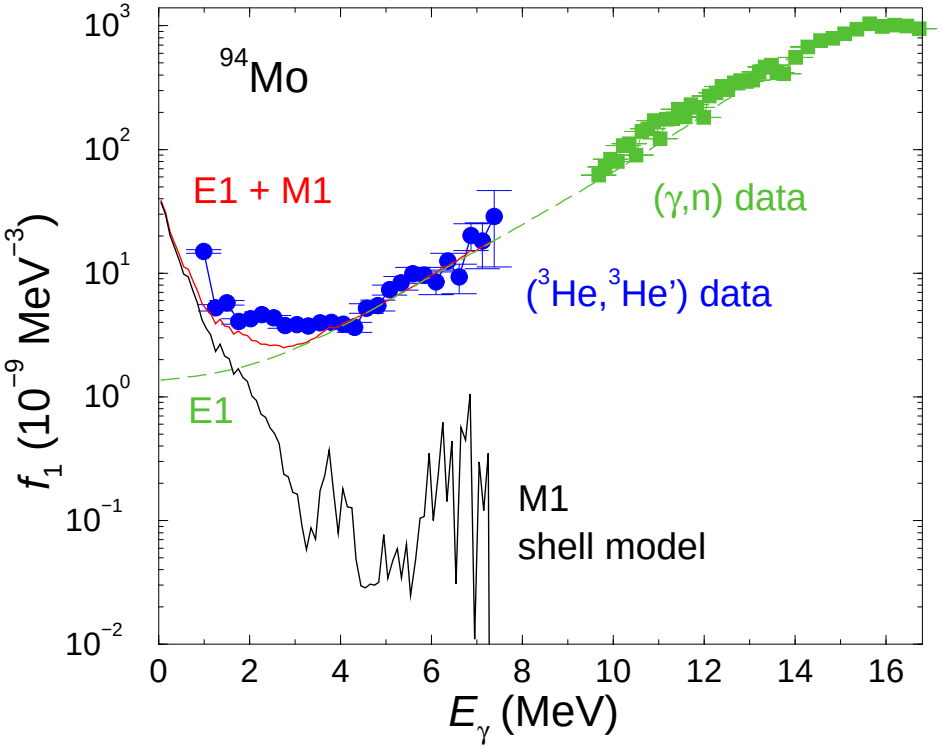

Low-energy enhancement of M1 radiation

RITSSCHIL

R.S., S. Frauendorf, A.C. Larsen
PRL 111, 232504 (2013)

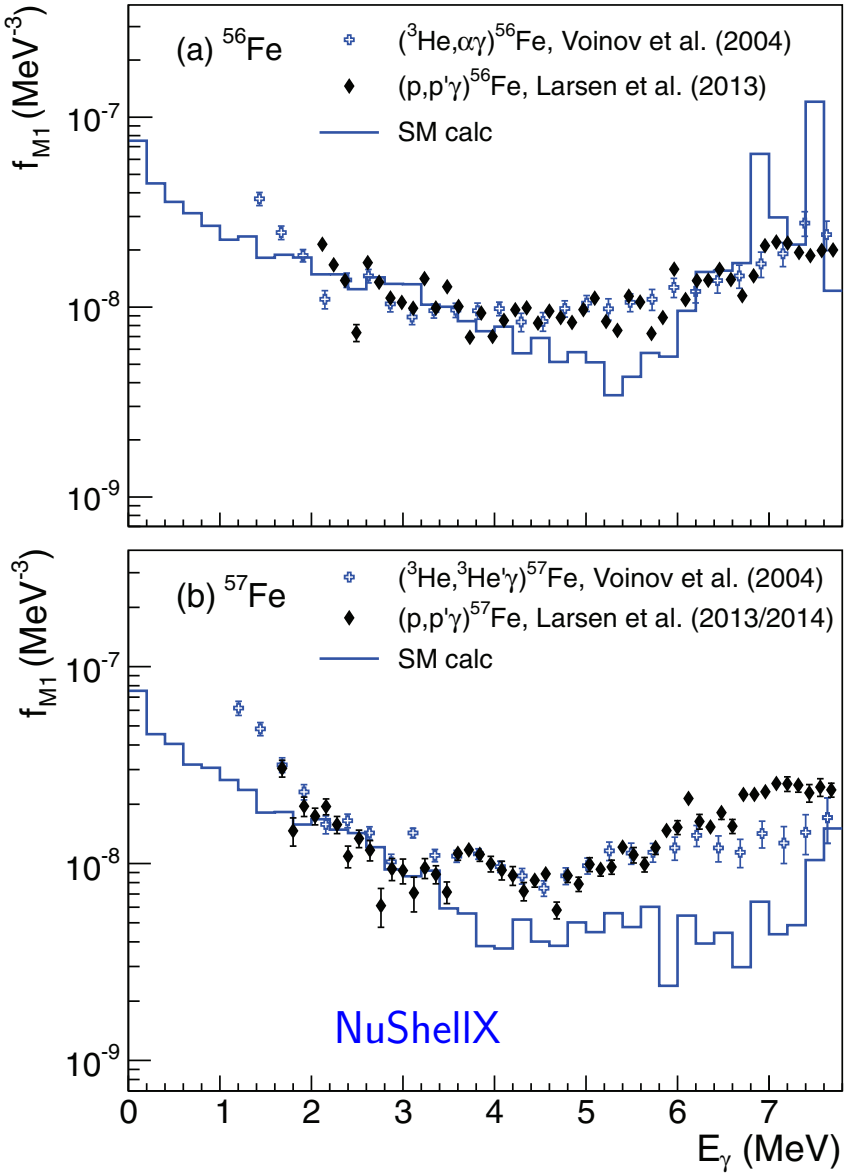

NuShellX

B.A. Brown, A.C. Larsen
PRL 113, 252502 (2014)

Average M1 strengths in Fe isotopes with N = 30 to 42

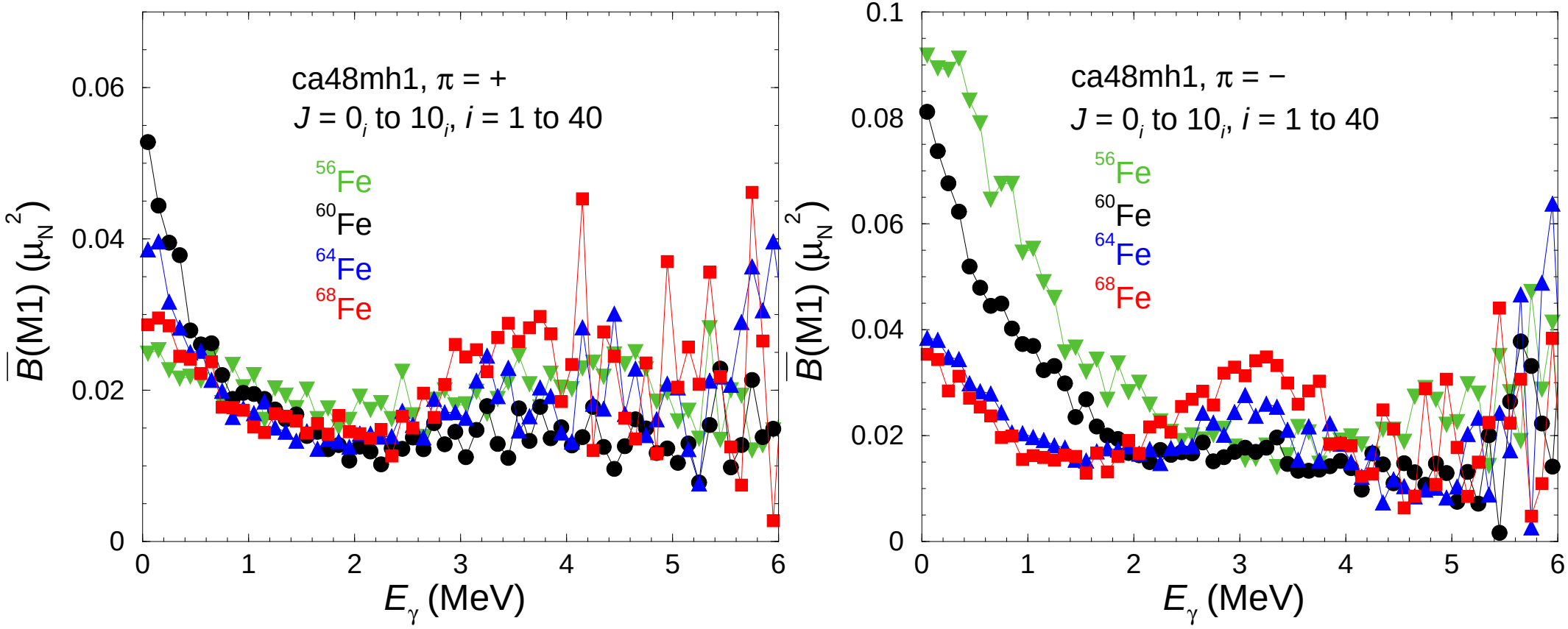

⇒ Enhancement of M1 strength toward very low transition energy.

⇒ Development of a bump around 3 MeV with increasing neutron number.

R.S. et al., PRL 118, 092502 (2017)

Dipole strength functions in ^{151}Sm and ^{153}Sm

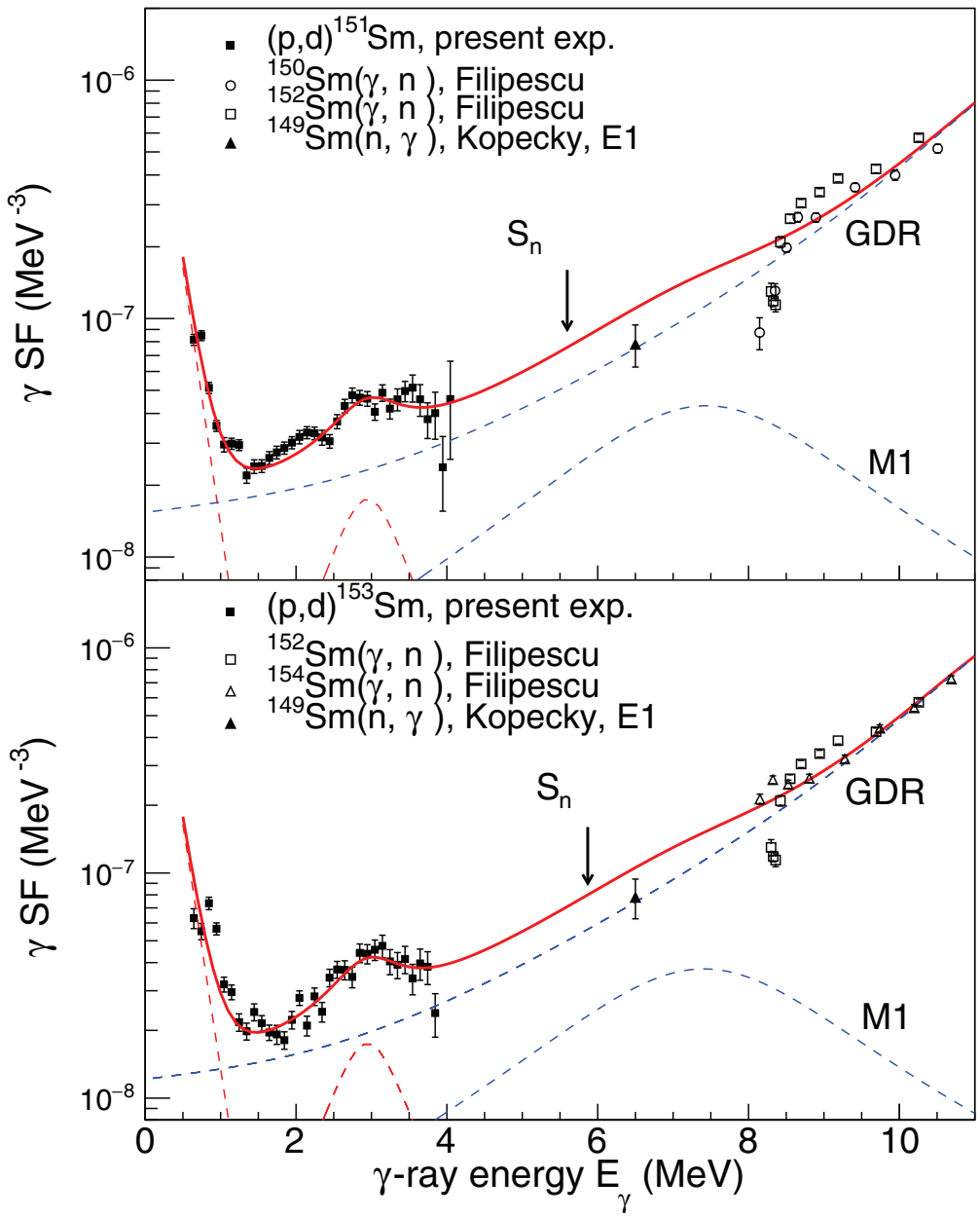

(p,d) data:

A. Simon et al.

PRC 93, 034303 (2016)

⇒ First observation of upbend and scissors resonance in one nuclide.

⇒ Strength in the scissors region about three times that found in (γ, γ) experiments.

Strength functions from shell-model calculations

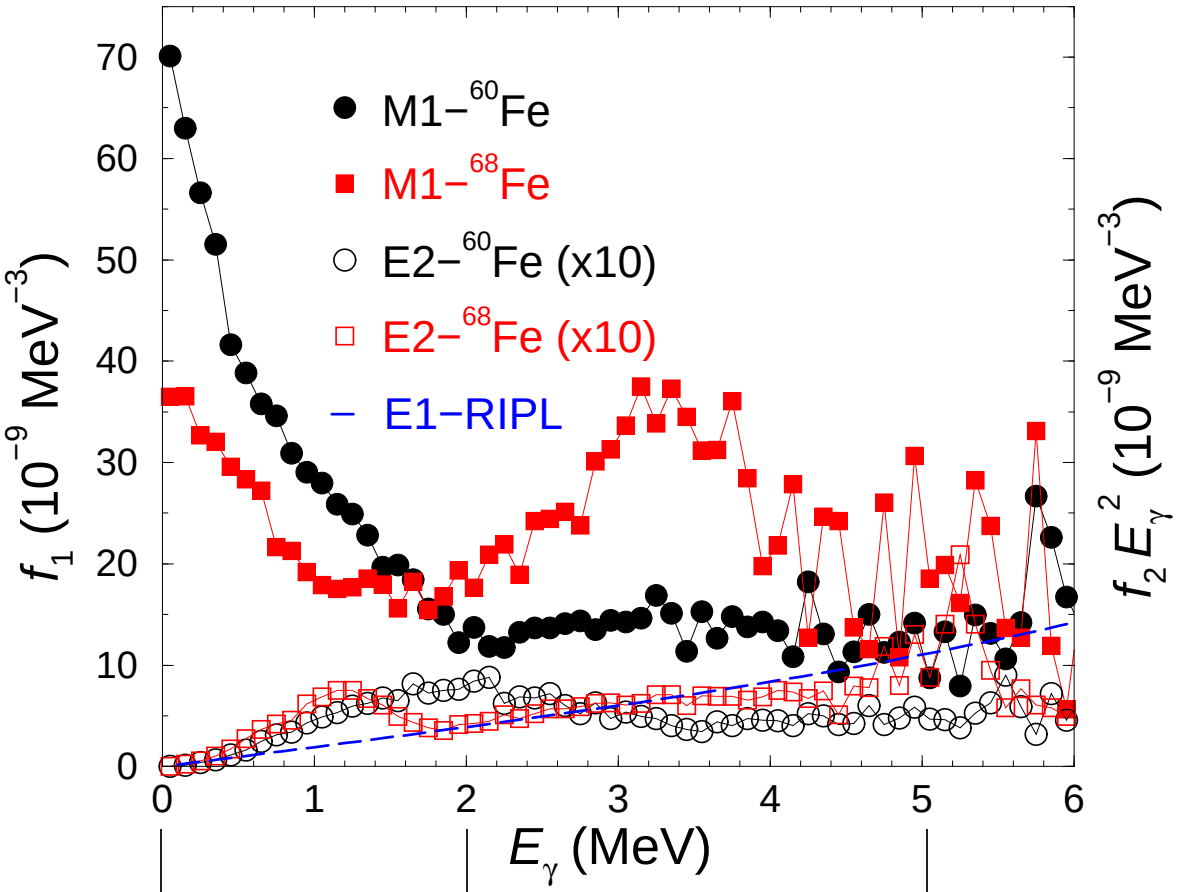

	$E_\gamma < 2$ MeV	$2 \leq E_\gamma \leq 5$ MeV	Sum
$^{60}Fe_{34}$	5.67	3.52	9.19
$^{64}Fe_{38}$	4.46	5.13	9.59
$^{68}Fe_{42}$	3.98	6.63	10.61

$B(\mathrm{M1})_{\mathrm{tot}}(\mu_N^2)$

Dipole strength function

$f_1 = 16\pi/9\ (\hbar c)^{-3}\ \overline{B}(\mathrm{M1})\ \rho(E_x, J)$

$\rho(E_x, J)$ - level density of the shell-model states, includes $\pi = +$, $\pi = -$, all spins from 0 to 10.

R.S. et al., PRL 118, 092502 (2017)

$\Rightarrow$ Strength in the scissors region about three times that found in (γ, γ) experiments.

Summary

- Photon-scattering experiments with broadband bremsstrahlung at γELBE and with quasimonoenergetic γ rays at HIγS up to the neutron-separation energies.
- Strength in the quasicontinuum of states included. Observed strength corrected for branching and feeding by means of statistical methods.
- Novel experimental information about the behavior of the full E1 strength in the pygmy region and the M1 strength in the spin-flip region for nuclides around masses 80, 130 and 180.
- Large-scale shell-model calculations of M1 and E2 strengths.
  - Description of the experimental low-energy upbend by enhanced M1 strength.
  - Correlation between the low-energy M1 radiation and the scissors mode in open-shell nuclei.
  - Explanation of different strengths found in photoexcitation and in light-ion reactions.

$\Rightarrow$ Modification of phenomenological strength functions used as input of statistical reaction codes needed.

$\Rightarrow$

Collaborators

Data analysis:	R. Massarczyk (HZDR/LANL) G. Rusev (HZDR/LANL)
Experiments at γELBE (HZDR):	D. Bemmerer, R. Beyer, R. Hannaske, A.R. Junghans, T. Kögler, A. Makinaga, K. Schmidt, A. Wagner *et al.*
Experiments at HIγS (TUNL):	C. Bhatia, M. Bhike, H. Kelley, E. Kwan, M.E. Gooden, R. Raut, A.P. Tonchev, W. Tornow
Calculations:	B.A. Brown (NSCL/MSU) F. Dönau (HZDR) S. Frauendorf (Notre Dame)